ELIMINATION OF PEARLITE-FERRITE BAND USING SOFT REDUCTION
DURING CONTINUOUS CASTING OF HSLA STEEL

A THESIS SUBMITTED TO
THE GRADUATE SCHOOL OF NATURAL AND APPLIED SCIENCES
OF
MIDDLE EAST TECHNICAL UNIVERSITY

BY

SADIK YETKİN

IN PARTIAL FULFILLMENT OF THE REQUIREMENTS
FOR
THE DEGREE OF MASTER OF SCIENCE
IN
METALLURGICAL AND MATERIALS ENGINEERING

JUNE 2014

Approval of the thesis:

ELIMINATION OF PEARLITE-FERRITE BAND USING SOFT REDUCTION DURING CONTINUOUS CASTING OF HSLA STEEL

submitted by **SADIK YETKİN** in partial fulfillment of the requirements for the degree of **Master of Science in Metallurgical and Materials Engineering Department, Middle East Technical University** by,

Prof. Dr. Canan Özgen   _____
Dean, Graduate School of **Natural and Applied Sciences**

Prof. Dr. C. Hakan Gür   _____
Head of Department, **Metallurgical and Materials Engineering**

Prof. Dr. Ali Kalkanlı   _____
Supervisor, **Metallurgical and Materials Engineering Dept., METU**

Prof. Dr. Ekrem Selçuk   _____
Co-Supervisor, **Metallurgical and Materials Engineering Dept., METU**

Examining Committee Members:

Prof. Dr. C. Hakan Gür   _____
Metallurgical and Materials Engineering Dept., METU

Prof. Dr. Ali Kalkanlı   _____
Metallurgical and Materials Engineering Dept., METU

Prof. Dr. Rıza Gürbüz   _____
Metallurgical and Materials Engineering Dept., METU

Prof. Dr. Bilgehan Ögel   _____
Metallurgical and Materials Engineering Dept., METU

Prof. Dr. Mustafa İlhan Gökler   _____
Mechanical Engineering Dept., METU

Date: 13.06.2014

I hereby declare that all information in this document has been obtained and presented in accordance with academic rules and ethical conduct. I also declare that, as required by these rules and conduct, I have fully cited and referenced all material and results that are not original to this work.

Name, Last name : Sadık YETKİN

Signature :

ABSTRACT

ELIMINATION OF PEARLITE-FERRITE BAND USING SOFT REDUCTION
DURING CONTINUOUS CASTING OF HSLA STEEL

Yetkin, Sadık

M.SC., Department of Metallurgical and Materials Engineering

Supervisor: Prof.Dr. Ali Kalkanlı

Co-Supervisor: Prof.Dr. Ekrem Selçuk

June 2014, 82 Pages

Line pipe steels are used to transport the crude oil and natural gas for the long range distances. The line pipe steel grades API X 60, API X 70 and API 80 defined by the American Petroleum Association are widely used by the line pipe manufacturers. The mechanical properties of the API grade steels are mostly affected by the segregation of alloying elements. Centre macro segregation is one of the most significant defects in continuous casting. This type of segregation causes the band structures through the steel coils. Therefore, if the cracks were occurred along these band structures, the cracks could easily move to the end of the line pipe following the band path. The most significant and effective method to reduce the macro segregation is the soft reduction which is the state-of-art of the continuous casting technology. The main aim of the soft reduction is to disperse the segregation of alloying elements using mechanical loading before the metallurgical length ends. By this way, the band structures caused by the macro segregation can be fully eliminated or reduced to negligible sizes. In this project, the soft reduction parameters are tried to find out the optimum parameters to eliminate the macro segregation for API X 65 5L PSL 2 steel grade. The micro structures of steel coils produced applied soft reduction are investigated and the band thicknesses of the coils are measured. In this research; the effect of soft reduction on the mechanical properties of final product is investigated.

Key Words: Soft Reduction, API X 65 5L PSL 2, Macro Segregation, Pearlite-Ferrite Band, Mechanical Properties, Mn Segregation

ÖZ

YÜKSEK MUKAVEMTLİ DÜŞÜK ALAŞIMLI ÇELİK KALİTELERİNDE OLUŞAN PERLİT-FERRİT BANTLAŞMALARININ SÜREKLİ DÖKÜMLER PROSESİNDE YUMUŞAK HADDELEME YÖNTEMİYLE YOK EDİLMESİ

Yetkin, Sadık

Yüksek Lisans, Metalurji ve Malzeme Mühendisliği

Tez Yöneticisi: Prof.Dr. Ali Kalkanlı

Ortak Tez Yöneticisi: Prof.Dr. Ekrem Selçuk

Haziran 2014, 82 Sayfa

Boru hatları; petrol ve petrolden üretilen ürünleri uzak mesafelere taşımak için kullanılan yöntemlerdendir. Petrol boru hatlarında kullanılan API X 60, X 70 ve X 80 gibi çelik kaliteleri Amerikan Petrol Birliği tarafından standartlaştırılmış olup boru hattı üreticileri tarafından yaygın olarak kullanılmaktadır. API grubu çeliklerin mekanik özelliklerini etkileyen en önemli unsurlardan bir tanesi alaşım elementlerinin segregasyonudur. Sürekli dökümler süreci boyunca oluşan segregasyonun en kritik olumsuzluğu alaşım elementlerin merkezde toplanmasıdır. Merkezde toplanan alaşım elementleri çelik bobinlerde perlit-ferrit gibi bant oluşumlarına sebebiyet vermektedir. Herhangi bir aksi durumda oluşan çatlaklar bu perlit bantları boyunca ilerleyip boru hatlarının çalışamamasına sebebiyet vermektedir. Son yıllarda geliştirilen ve en son mühendislik çalışmalarına konu olan yumuşak haddeleme sürekli döküm süreci esnasında uygulanmakta olup segregasyonu dağıtmak için en etkin yöntemlerden bir tanesidir. Yumuşak haddelemenin temel prensibi sürekli döküm esnasında çelik slablar tamamem katılaşmadan uygulanıp ortada toplanan alaşım elementlerini slab içerisinde dağıtmaktır. Böylece alaşım elementlerinin segregasyonundan kaynaklanan perlite-ferrit gibi yapılaşmaları en aza indirgemek veyahut yok etmektir. Bu projenin temel amacı; API X 65 5L PSL 2 çelik kalitesinde yumuşak haddeleme yöntemi kullanılarak sürekli dökümler esnasında oluşan alaşım elementlerinin segregasyonu önlemek ve en uygun değişkenleri bulmaktır. Bu amaca ulaşmak için; yumuşak haddeleme yöntemi uygulanan çelik bobinlerin mikro yapıları incelenmiş olup bant kalınlıkları

ölçülmüştür. Son olarak çelik bobinlerin mekanik özellikleri yumuşak haddelemenin etkisini görmek için incelenmiştir.

Anahtar Kelimeler: Yumuşak Haddeleme; API X 65 5L PSL 2 Çelik Kalitesi, Alaşım Elementlerinin Segregasyonu, Perlite-Ferrit Bantlaşması, Mekanik Özellikler, Mangan Segregasyonu.

To My Parents

ACKNOWLEDGEMENTS

TABLE OF CONTENTS

LIST OF TABLES

TABLES

LIST OF FIGURES

FIGURES

XVII

CHAPTER 1

INTRODUCTION

Natural resources such as nation's crude oil and natural gases are basically the raw materials for energy of the world consumes. Unfortunately; these resources are located in exceedingly different regions than they are processed or refined into fuels for human beings. Pipelines are simply the intermediate process that moves the product from the oil fields to the marketplace. The marketplace can be refineries, manufacturers and distribution centers. Energy (or petroleum) pipelines play significant role on daily life of human beings and the nations' economy. For instance; pipeline systems are admitted as either the safest transportation mode or the most economical way of distributing the enormous quantities of oil from production fields to refineries or from refineries to consumers. According to American Petroleum Institute data the oil pipeline network alone in the U.S. is more than 10 times larger than that in Europe. The pipelines operate every day with the help of powerful pumps, oil additives that move the oil with less resistance and the laws of physics. Through a single pipeline dozens of products and grades of gasoline such as regular gasoline, premium gasoline, diesel, jet fuel at once can be transported. This process is named as "Batching". This process makes possible through one single pipeline to distribute the energy needs for the nation. Some mixing occurs at the point where the batches touch; especially at junction points. This mixture, called "transmix," is removed and reprocessed from the pipeline at the receiving facility. These kinds of processes and mixtures extremely decrease the service life of pipeline materials for the reason that these mixtures containing hydrogen sulphide are very corrosive for the steel. Another factor affecting the service life of pipelines is cracks. Unless the maintenance of pipeline is done properly; cracks will go likely unnoticed. The replacement of the pipeline is very

expensive and sometimes challenging at fields considering winter time. The pipeline materials are chosen by end users according to the standards of American Petroleum Institute (API) which has been operating the standards for the oil and natural gas industry since 1924. The American Petroleum Institute has determined the steel grades for the use of pipelines such as API X 65, API X 70 and API X 120 etc. The product characteristics of these steel grades are mainly ultra- high strength steels, excellent low temperature toughness and good corrosion resistance for hydrogen induced cracking. Hydrogen induced cracking (HIC) named also as hydrogen embrittlement is significant factor that determines the service life of pipeline. The basic mechanism of HIC is the diffusion of atomic hydrogen through the steel. When the steel is saturated with atomic hydrogen that re-combines in microscopic voids of the steel; they create the pressure from the voids that are located inside. The pressure can be increased up to yield strength of steel. Therefore; the cracks are formed. The API X steels grades have ferrite morphology. The hydrogen emissivity of ferrite is 10 times higher than pearlite. This is one of the reasons of API X steels grades are used in pipelines. In other words; the pearlite morphology is considered as defect. The pearlite bands are formed due to the segregation of carbon and manganese during hot rolling process. To eliminate the pearlite morphology from steel coils from several decades so many researches have been done. However; during mass production the elimination of pearlite-ferrite bands is very tough question. Recently; soft reduction technology is invented during continuous casting to disperse the carbon and manganese segregation.

In this research the API X 65 steel grade is chosen and to eliminate the pearlite-ferrite band the soft reduction technology is used. Almost 100 steel coils are manufactured using different soft reduction ratio. 11 samples were chosen to investigate the pearlite-ferrite band. The pearlite band thickness is measured and compared. In addition; the pearlite morphology of the samples are investigated using scanning electron microscopy. Finally; the mechanical properties of samples are compared with each other to see the effect of soft reduction.

CHAPTER 2

LITERATURE REVIEW

2.1) Continuous Casting

Continuous casting is the greatest improvement in the history of steel casting. There are two types of continuous casting technology. [32, 35]

2.1.1) Conventional Continuous Casting

The aim of conventional continuous casting is to produce the thick steel slabs and delivery the slabs to the slab yard or to the reheating furnace and rough rolling process. The slab thickness produced by conventional continuous casting is constant and varies between 200 and 250 mm according to machine capacity.
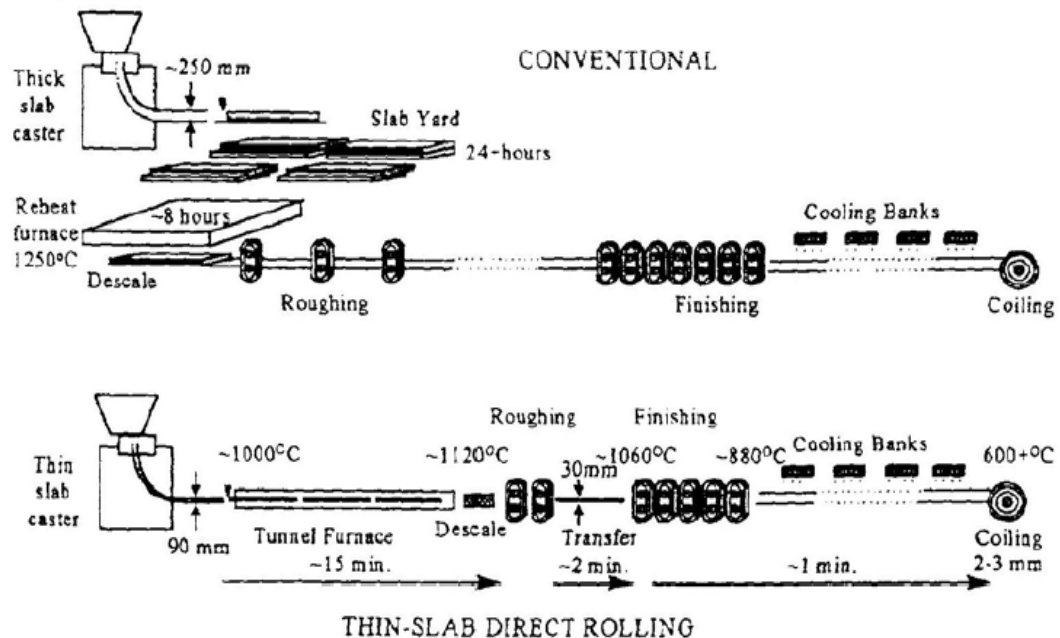
Figure 2.1 The schematic views of conventional and thin slab continuous casting processes [32]

2.1.2) Thin Slab Continuous Casting

The thin slab continuous casting technology is the evolution of the compact strip production which was invented by Nucor Steel in 1986. The thin slab continuous casting technology is the integrated system of solidification and liquid core reduction. The solidification starts in the mould which is same with the conventional casting. The thickness reduction is done by the process of liquid core reduction while the centre of slab is in the liquid state. The aim of this system is to produce the thin slabs. The slab thickness produced by thin slab continuous casting is changeable during process and varies between 50 and 90 mm. The decreased thickness makes the rough rolling process more easily and in shorter time comparing conventional continuous casting. This system also requires the reheating process. However; this reheating process is the integrated to the rolling process called tunnel furnace. The process time of reheating is between 15 and 30 min depending on the dimensions of casted steel. This direct charging and decreased heating makes the thin slab casting process economically favourable. Another advantage of thin slab casting is that decreased reheating time limits the grain growth, dissolution of precipitates. The rapid solidification of thin slab compared to conventional casting technology makes the dendritic structure more refined and this contributes to greater homogeneity because of liquid core reduction. However; the system has disadvantages comparing conventional continuous casting. First and foremost disadvantages is that any significant problem occurred on the continuous casting line makes to stop the whole production line. For instance; the sticking problems during casting process stop the whole production line between 1 hour and 10 hour depending on the damages. To prevent the sticking problem requires significant engineering work and casting experience. Engineers and casting operators on the thin continuous casting should be very well educated. Secondly; the quality of liquid steel is so important that the production stops because of nozzle clogging. To illustrate; because scraps contain of impurities, copper and tin alloys; % 100 scrap steel used as raw material for thin slab continuous casting is not suggested. The thin slab continuous casting is usually suggested to the companies which has blast furnace. Thirdly; scale formation is higher during reheating furnace on the conventional casting than during the tunnel furnace on the thin slab continuous casting. This thick scale makes to remove the

surface defects more easily and cleanly. After descaling process the thin slabs should be investigated more carefully compared to the thick slabs. In addition; some steel grades; such as peritectic steel grade or Nb alloyed steel grades, are more prone to transverse crack formation produced by the thin slab continuous casting because of hot ductility problems [6,7,25,26].

2.2) High Strength Low Alloy Steels: HSLA

High strength low alloy steels are defined as micro alloyed steels. The main purpose of high strength low alloy steels is to provide the desired mechanical properties or the greater resistance to corrosion like more suitable for the application of coatings. HSLA steels are not classified in the alloy steels category; in fact they are individually considered as a separate steel group. These steels generally contain maximum 0.12 % carbon and 2.1 % manganese contents that provides excellent weldability and formability. By this way; they are suitable to manufacture the structural components such as crane components and platforms, urban lighting masts, industrial vehicles. HSLA steels generally contains of small amount of alloying elements like mainly titanium, vanadium, boron, niobium. The small alloying addition makes the steel hardened by a combination of precipitation and grain size refining. Hence; HSLA steels do not exhibit either weld zone softening or grain coarsening. To illustrate more clearly; the small amount addition of niobium or titanium like < 0.10 % increases the strength of steels. This enhances to decrease the carbon content of steel. By this way; the weldability of steel increases. In terms of coating; the additions of alloying elements are generally maximum 0.20 %. This small amount of alloying elements does not cause any problem for the coating. For instance; in some cases the thickness of the coating can be up to 2 mm for HSLA steels. This coating characteristic makes the HSLA steels favorable for the automotive industry like body chassis or suspension systems. HSLA steels are generally classified according to their yield strength. For example; according to the EN 10149-2 standard S 315 MC steel is classified based on the yield strength minimum 315 MPa. In this research; API X 65 steel grade is investigated [36].

The American Petroleum Institute (API) determines the standards to manufacture the line pipes suitable for use in transporting the water, gas and oil for

especially long range distances in both the oil and the natural gas industries. These specifications like 5L includes the chemical analysis, mechanical testing (tensile, bending, Charpy toughness and hardness), macro- and microscopic testing of welds, hydrostatic testing and visual non-destructive testing regarding the particular application and operating conditions.

There are 2 types of product specification level PSL 1 and PSL 2 for the API 5L steel grades. PSL 1 defines the basic requirements such as chemical composition and minimum yield or tensile strength whereas PSL 2 defines the enhanced requirements including mandatory notch toughness, restricted strength ranges, carbon equivalents for improving weldability. According to API standard X65 5L; the carbon equivalent should be less than 0.43 %. In addition; the sum of niobium, vanadium and titanium shall be 0.15 %. The impact energy at 0ºC should be minimum 27 Joule.

Table 2.1 Mechanical Properties of API Steel Grades according to PSL 2 Pipe

Pipe Grade	Yield Strength				Tensile Strength			
USC/ SI	Min (ksi)	Min (MPa)	Max (ksi)	Max (MPa)	Min (ksi)	Min (MPa)	Max (ksi)	Max (MPa)
L360/ X52	52	360	76	530	67	460	110	760
L415/ X60	60	415	82	565	76	520	110	760
L450/ X65	*65*	*448*	*87*	*600*	*77*	*531*	*110*	*758*
L555/ X80	80	555	102	750	60	621	120	827
L690 / X100	100	690	121	840	110	760	143	990
L830 / X120	120	830	152	1050	132	915	166	1145

Table 2.2 The chemical composition of API 5L X65 steel grade

	C	Mn	Si	S	P	Nb	Ti	V	Ni	Cr	N
Min	0,05	1,45	0,10	0	0	0,035	0,015	0,02	0	0	0
Max	0,08	1,60	0,20	0,008	0,015	0,050	0,025	0,04	0,10	0,05	0,009

The types of inspections required are based on the product form and the specification level and include;

    a) Visual for Defects and Dimensions Inspection
    b) Radiographic Inspection
    c) Electromagnetic Inspection
    d) Ultrasonic Inspection
    e) Magnetic Particle Inspection
    f) Hydrostatic Testing
    According to Product Specification Level 2 Carbon Equivalent:
    $C_{eq} = C + Mn/6 + (Cr+Mo+V)/5 + (Ni+Cu)/15$

$$(1)$$

The API 5L X65 steel grade is in the category of high strength low alloy steels (HSLA). To illustrate more clearly, API 5L X65 steels consist of the small amount of alloying elements like Nb, Ti and V which gives the X 65 steels more the mechanical resistance, toughness at low temperatures (less than 0°C), weldability and resistance to embrittlement to related to hydrogen. By this way, these API 5L X65 steels can be presented to enhance the reliability in the operation the line pipes in the hostile environments. In this project API 5L X65 steels are investigated. The main reason preferring the API 5L X65 is the most widely used steel grade [11].

2.3) Metallurgical Problems Associated with Formation of Pearlite-Ferrite Band in Petroleum Pipeline

Pearlite-ferrite band formed in the centre line of coils is undesired micro structure for several decades. This band structure mainly causes the crack formations and

developments on the steel coils. There are 3 main cases that explain why the pearlite-ferrite bands are not desired especially for petroleum pipe lines. First and mostly encountered case; during welding process of petroleum steel pipes cracks are formed where the welding zone and pearlite-ferrite bands are combined. These cracks are mainly detected by the ultrasonic testing. Secondly; cracks initiated by any kinds of impacts on the petroleum pipes go along the pearlite-ferrite band. In some cases this kind of crack lengths is 1-2 m. The replacement of the pipe line and the loss of the raw material are devastating not only for companies and end users of petroleum products. Last case is that the petroleum pipe lines carry many kinds of liquids and gases on the long distances. One of these gases is H_2S which is very corrosive. The hydrogen gas is one of the reasons for degradation of mechanical properties of pipeline steels. The corrosion caused by hydrogen gas decreases significantly the service life comparing the expected life[3,8,12,13,14,15,27,28,29,30].
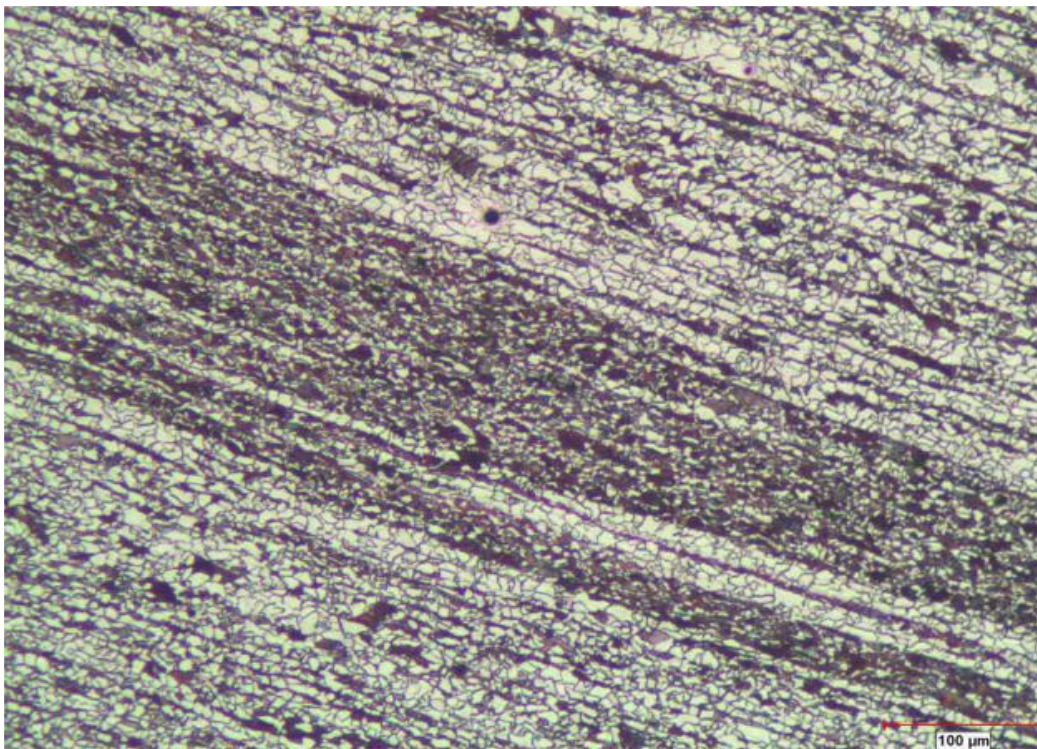
Figure 2.2 St 52 Steel Grade Pearlite-Ferrite Band

Figure 2.3 X70 Steel Grade DWTT Testing Sample Crack goes along the pearlite-ferrite band.

The macro segregation of manganese and carbon during continuous casting causes the formation of pearlite-ferrite band. The formation mechanisms of manganese and carbon are completely different from each other. To start with the manganese segregation; the steel casting temperature is between 1530℃ and 1540℃ for continuous casting. The melting temperature of manganese is 1246℃. The composition of manganese for this research is 1.50 -1.60 % (in mass percent). All manganese is soluble in casting temperature range. During continuous casting steel solidifies from outer surface to inner surface. When the steel starts to solidifies; the solid steel rejects the manganese to the liquid steel. In the centre liquid becomes manganese rich. This process continues until the centre liquid solidifies. By this way; in the centre of slab the solid becomes manganese richer than in the outer surface of slab. Manganese not only lowers the eutectoid temperature and composition but also decrease the chemical activity of carbon in austenite during hot rolling process. In other words; the manganese swifts the pearlite transformation line to the left in TTT diagrams. This causes the pearlite formation rather than ferrite formation. To continue with the carbon segregation; the maximum carbon solubility

of the austenite is 2.11 % C around 1148℃. The maximum solubility of ferrite is 0,028 % C around 728 % C. The solidification continues from outer to inner during continuous casting. The average temperatures are around 900 ℃, 1100 ℃ at the corner and sides of the slabs, respectively during continuous casting. Liquid steel still exists inside slab during continuous casting. The microstructure of slab continues from the ferrite at the corners to austenite under the surface and lastly carbon rich liquid steel during continuous casting. Carbon rejection from ferrite to austenite microstructure causes being carbon rich liquid which solidifies and becomes carbon rich ferrite lastly at the centre of the slab. The carbon rich ferrite forms the pearlite during continuous cooling of hot rolling process. This kind of pearlite band can be eliminated in 2 different ways in the view of scientific manner. First one is that the slabs should be heated prolonged time around 1200 ℃ and apply the extensive hot working to homogenize the steel with the respect to manganese. Second is that slab should be heated short time around 1400 ℃ which allows the carbon diffusion but not the manganese diffusion. These ways are not practical for serial production of steel coils. [21, 22, 23, 24]

2.4.) Solutions to Eliminate Pearlite-Ferrite Band Formation in Continuous Casting of HSLA Steels

The elimination of pearlite-ferrite band formation is very tough question in steel industry. Because there are three main ways to avoid the macro segregation of manganese and carbon and eliminate the pearlite-ferrite band structure during continuous casting process. The adaptation of these ways to the continuous casting machines is not such easy. To illustrate this phenomena; these 3 ways are described in detail below;

2.4.1) Electromagnetic stirring (EMS):

Electromagnetic Stirring can be basically defined as stirring the liquid steel creating electromagnetic field during continuous casting. Stirring liquid steel breaks the secondary arm dendrites during solidification. By this way; the alloying elements

can be distributed more uniformly and there is more time for equiaxed grains solidify. Electromagnetic stirring units can be installed to the continuous casting mould; secondary cooling zone and the final solidification zone. The most and least effective zone for electromagnetic stirring is the mould and final solidification zone, respectively. The effect of electromagnetic stirring on the quality of the semi-finished products during continuous casting depends on the stirring of liquid steel. Increase the thickness of solidified shell decrease the liquid steel and decrease the effect of electromagnetic stirring. In addition; the effect of the electromagnetic stirring is directly related to the casting speed. To illustrate the casting velocity relation; the stirring becomes more effective at higher casting velocities because of liquid turbulence. The casting velocities of billet and slab castings are maximum 5.0 m/min and 1.6 m/min, respectively. The EMS can be very effective method to decrease the macro-segregation for billet casting. On the other hand; this technology is not very effective for the application of slab castings. [21]

2.4.2) Liquid Core Reduction:

Liquid core reduction is the essential part of thin slab casting technology. To illustrate the liquid soft reduction; generally the thin slab casting machines have casting mold and 7 segments. The segments have guide rolls with adjustable gaps and sensors fitted to control the slab thickness. Liquid core reduction is applied in the first one segment or first two segments depending on the steel grade and desired thickness reduction. The thickness of the slab after casting mold is 90 mm. The thickness of the slab; which has liquid steel in the center, is decreased from 90 mm to 70 mm by mechanical force of segments. Otherwise; if the center is solidified; the enormous mechanical forces are required to make the same reduction. This reduction; which varies from 25 to 40 % in thickness, makes secondary dendrites break. By this way; the more equiaxed grains are formed. In addition; the liquid core reduction has significantly more refined columnar zone which can cause the cracks during continuous casting. According to previous researches; the liquid core reduction significantly decreases the grain size from 150 μm to 50 μm. However; any effect on the segregation of alloying elements are not observed [7].

2.4.3) Soft Reduction:

Considering the current technologies; the soft reduction is the state-of-art of the continuous casting process because the soft reduction is the easiest and most effective way to reduce the macro segregation and the presence of central casting cavity for the conventional continuous casting. By this way; the internal quality of the castings can be improved. To illustrate the soft reduction; it can be considered as "Soft Rolling Operation" before the solidification ends during the continuous casting. In other words; the applied certain amount of force during the continuous casting prior to the final point of solidification eliminates the casting cavity and disperses macro segregation along the centre line of the casting [17, 18, 19, 20, 34].
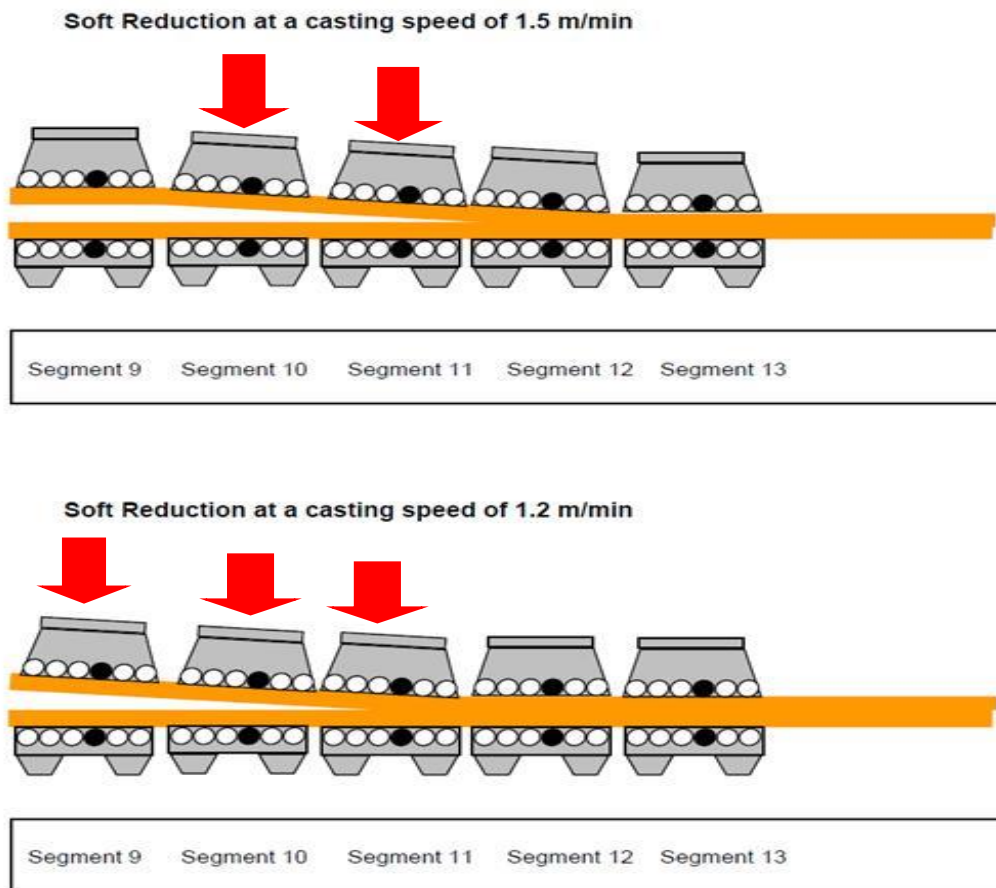
Figure 2.4 Schematic View of Soft Reduction during Continuous Casting

12

Soft reduction depends mainly on the steel composition, metallurgical length and casting speed. To begin with steel composition; the applied force by soft reduction depends on the steel strength which strictly depends on the steel composition. In addition; the solid wall thickness of slab during continuous casting should be investigated carefully. There are two important reasons. The first and foremost reason is that the strength of the slab during continuous casting strictly depends on the thickness of the slab. To illustrate this reason; the soft reduction can be defined such that the soft reduction breaks the zero strength dendrites using the ferro-static pressure. By this way; the equiaxed solidification region expands during continuous casting. The benefit of the equiaxed solidification prevents the casting cavities. The second significant reason is that the solid wall thickness of the slab is near the final thickness of the slab and the liquid steel may not break the dendrite during continuous casting; there is no time for liquid to penetrate between the dendrites. The importance of liquid steel during continuous casting comes from unsolved alloying elements such titanium, niobium or manganese. The dispersion of unsolved alloying elements in liquid steel is great importance on the mechanical properties of the final product. For instance; the uneven dispersion of unsolved alloying elements cause the unexpected cracks during hot rolling. The manganese dispersion is the important factor on the pearlite-ferrite band formation. That is why the application zone of soft reduction plays great role on the success of reducing the pearlite-ferrite thickness. Secondly; the soft reduction should be applied before the metallurgical length ends. Because the soft reduction works on the principle of hydro-static pressure of steel liquid which break the secondary dendrite arms.
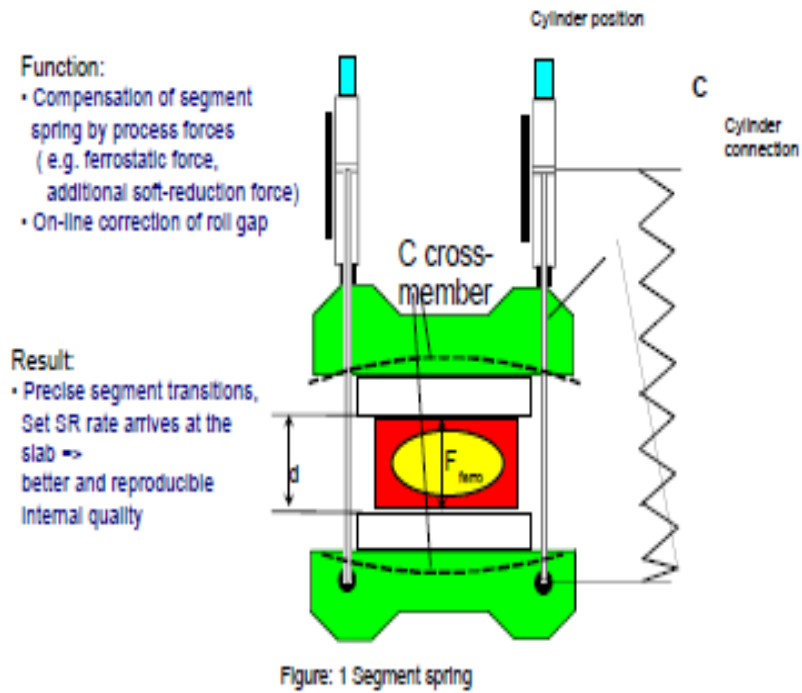
Figure 2.5: Soft Reduction Segment [17]
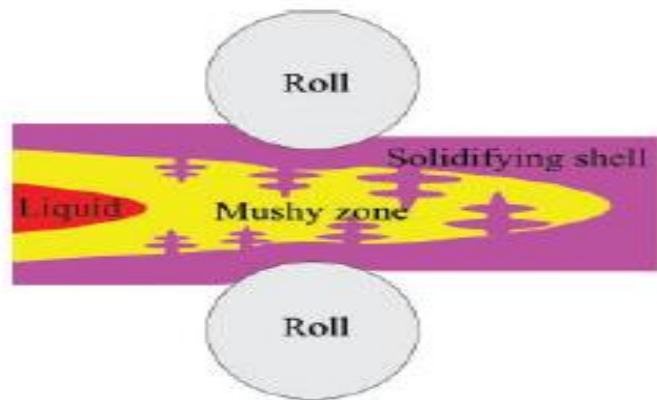
Figure 2.6: Schematic diagram of soft reduction by pinch rolls [38].

As shown in Figure 2.6; during continuous casting operation there are 3 main phases regarding liquid, mushy zone and solidified shell in the slab. The solidified shell is mainly austenite and the outer temperature of the solidified shell is between 1100 ℃ and 900º C during continuous casting.
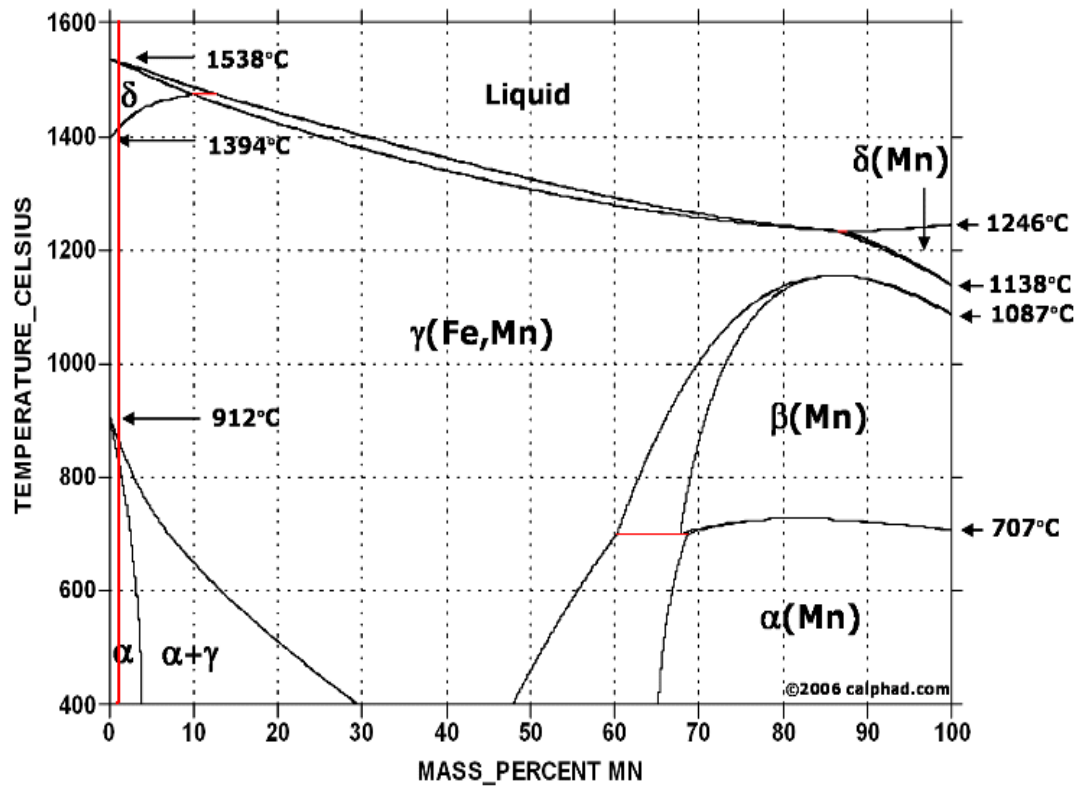
Figure 2.7: The Fe-Mn Phase Diagram [41]

The liquid; which is around 1500 ℃, is alloying enriched. The most significant alloying element regarding API X 65 grade steel is manganese. The mass percent of manganese in API X 65 steel is around % 1.5. The maximum solubility of manganese at 1529 ℃ is 10 % in mass percentage and the phase is delta ferrite. The manganese solubility of the delta ferrite decreases up to 0 while the temperature decreases up to 1394 ℃. During solidification of steel, the manganese element is rejected from solidified dendrite to the liquid. By this way; the liquid becomes alloying enriched. The mushy zone consists of both dendritic region and alloying enriched liquid. The tips of the dendrite are delta ferrite and the main body of the dendrite is austenite [39]. In mechanical point of view; the dendrites consist of zero

15

strength zone surrounded by alloying enriched liquid, liquid impenetrable zone that has enough strength to resist the ferro-static pressure of liquid and zero ductility zone [40].
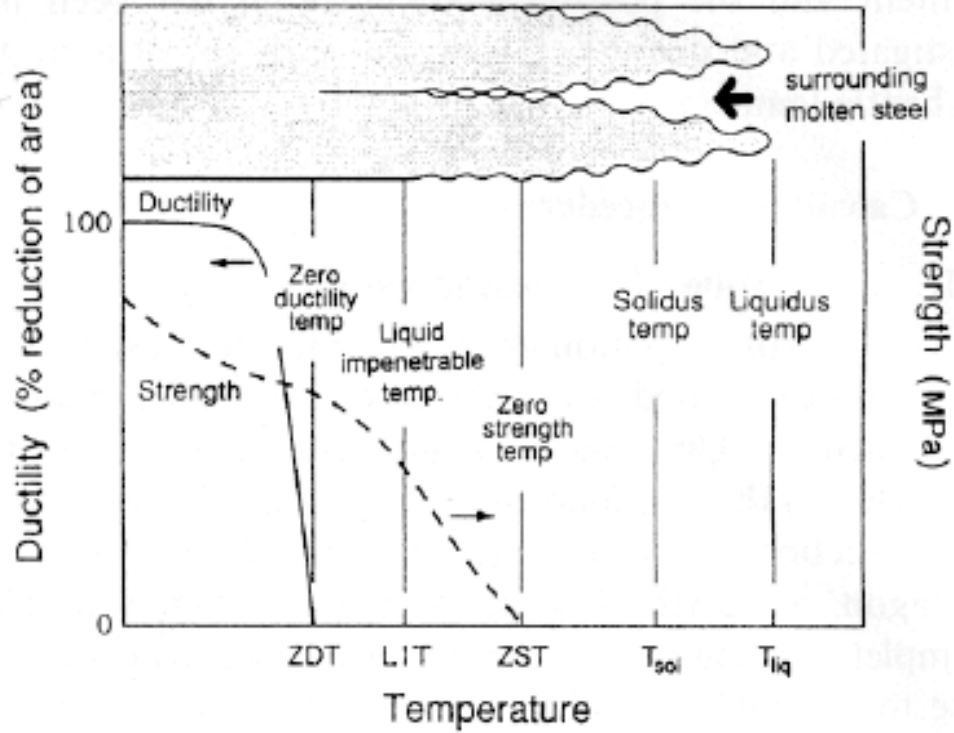
Figure 2.8: Mechanical properties in the high temperature zone of reduced ductility and corresponding presentation of solid/liquid interface during casting [40]

When soft reduction is applied to the slab during continuous casting, the mechanical force of the soft reduction breaks the zero strength part of the dendrites up to the liquid impenetrable part. In addition; the alloying enriched liquid can penetrate through the liquid impenetrable part of the dendrites because of the ferro-static pressure caused by soft reduction. To achieve this phenomena; it is so important to determine the solid fraction.

16

According to the research of Mr. Liu and Mr Zhang [19]; the solid fraction (f_s) as a function of temperature can be calculated from the following equation;

$$f_s = \frac{T_s - T + \frac{2}{\pi}(T_s - T_l)\{1 - \cos[\frac{\pi}{2} * \frac{(T - T_s)}{(T_s - T_l)}]\}}{(T_l - T_l)[1 - \frac{2}{\pi}]}$$

(2)

T_s is the temperature of solid in the mushy zone.

T_l is the temperature of liquid in the mushy zone.

T is the pouring temperature of liquid.

f_s is the temperature dependent solid fraction of steel in the mushy zone.

CHAPTER 3

EXPERIMENTAL PROCEDURE

3.1) Materials and Processing

The API X 65 specification PL 2 standard steel grade was used in this study. To manufacture the slabs the continuous casting process was applied. The number of manufactured slab was 110. The samples were taken from 11 different slabs. The chemical compositions are listed in Table 2.1. The chemical composition was determined to catch the carbon equivalent % 0.43. In the view of the elements S and P great damage to the toughness, these contents (in mass percentages) were limited 0.0025 % and 0.020 % respectively. The brand of continuous casting machine is SMS Demag which has 2 strands in Isdemir. The samples were chosen from the same strands. The slab dimensions were 225 mm thickness and 1517 mm width. The casting temperature varied between the 1540°C and 1560°C. The casting speed and soft reduction ratio (mm/m) were changed during continuous casting process. The casting speed and soft reduction ratio are listed in Table 2.2.

The thermal taper was determined as 0.2 mm/m. according to the previous experiments that is the measured gap distance between enter and exit without soft reduction. In addition; comparing the previous experiments and considering 0.2 mm/m. thermal taper the soft reduction ratio was determined and listed in Table 2.2. In other words; for instance; the soft reduction ratio is determined 1 mm/m. The thermal taper of API X65 steel grade is 0.2 mm/m. The total reduction ratio is 1,2 mm/m. After the continuous casting process; the hot rolling process was applied to the slabs. The charging method to the per-heating furnace was cold. In other words; the charging temperature of the slabs was 25°C. The coil dimensions are 12 mm thickness and 1500 mm width. The slab temperature after preheating furnace was 1230°C and the holding time during preheating furnace was 2.5 hours. The rough

rolling temperature was around 1020°C. The finish rolling temperature was around 820°C. The coil rolling temperature was around 540°C.
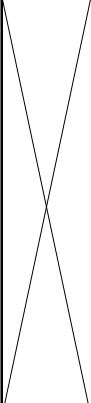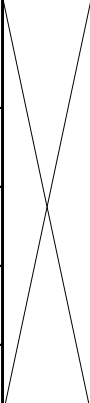
3.2) Macro- and Micro-Structural Investigations

To investigate the casting cavities in the slabs the macro-samples were taken from the end of the slabs. After the slabs were air-cooled, the macro-samples were taken from the slabs. The dimensions of the macro-samples are 150 mmx225mmx30mm. The macro-samples were cut in 2 different directions; perpendicular to the casting direction and parallel to the casting direction. To get the smooth surface; the macro-samples were machined in CNC Milling Machine. After machining; the macro-samples were cleaned using the %10 HCl acid-pure water concentration during 50-60 minutes to remove the machining oil and rusts.

To investigate the pearlite-ferrite bands the samples were taken from the centre line of the coils. The sample dimensions were 10 mmx10 mmx12.35 mm. After the samples were applied to the grinding, polishing, the samples were etched in %3 Nital solution in 15 seconds. The X25 micro-structure figures were taken to investigate the distribution of the pearlite-ferrite bands. In next step; the pearlite-ferrite band thicknesses were measured from the 100X micro-structure figures using Materials Plus software program. The linked pearlite band; which can include the ferrite grains or not, are measured 5 times from different locations along the casting direction. There are two purposes that linked pearlite bands are taken into consideration. First one is that the weakest points of the coils are these areas if any cracks occur or any welding meets the pearlite bands. Secondly; when the pearlite band including ferrite grains is imagined at 3D view, the pearlite grains can be under the ferrite grains. For instance; if pearlite band is re-grinded, the thickness of band can be both thicker and thinner. That is why the linked pearlite bands including ferrite grains are considered in this project. At last step, according to the ASTM E112-96 the grain sizes were calculated.

3.3) Mechanical Testing Investigation

The tensile testing, impact energy testing, DWTT testing and hardness test were carried out according to the API 5L PSL 2 standard. The mechanical testing samples were cut between the last 8 meter and 5 meter from the coils. The wide of the coils were 1500 mm. The 150 mm (1/10 of cut coil sample) wide was cut away from both sides. The schematic view of the samples; in which was taken from the coil, was drawn in the figure. The samples were taken from both sides of the coils. The dimensions and average values of the test samples are written in the mechanical testing results list. The thickness of all testing samples was same and around 12 mm for the tensile testing. To make the samples same thickness for the tensile testing; the samples were machined in universal grinding machine. The Vickers hardness test using 5 kg load was applied. The Vickers hardness testing samples were taken from the centre line of the coil. The number of the hardness testing value was taken 2 from the both bottom and top side.

1/10 Cut		1/8	1/8	1/8	1/8	1/8	1/8	1/8	1/8		1/10 Cut
		Tensile Testing Sample			Mechanical Testing Samples were not taken		Tensile Testing Sample				
		Impact Energy Sample					Impact Energy Sample				
		Impact Energy Sample					Impact Energy Sample				
		Impact Energy Sample					Impact Energy Sample				
		DWTT Sample					DWTT Sample				

Figure 3.1 Mechanical Testing Sample Preparation from Coil
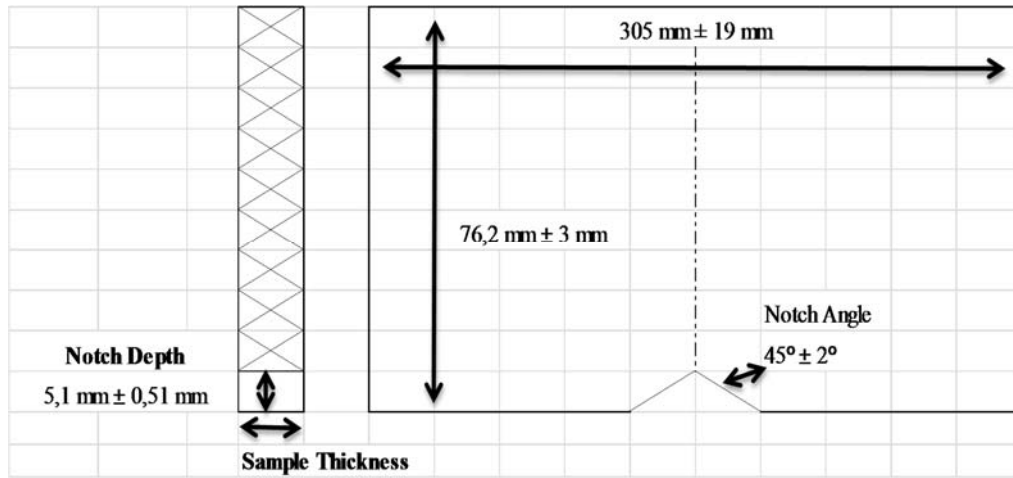
Figure 3.2 DWTT Sample Dimensions

Figure 3.3 Pragya DWTT
Testing Machine

Figure 3.4 Pragya DWTT Sample
Preparation Machine

The DWTT testing machine is Pragya. The maximum height is 3.80 m. and the maximum weight is 1400 kg. The DWTT testing samples were held 2 hours at 0°C refrigerator.
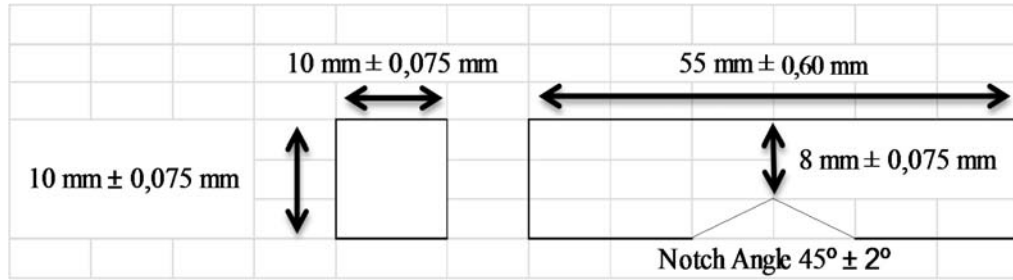
Figure 3.5 Impact Energy Testing Sample Dimensions

Figure 3.6 Zwick/Roell Impact
Energy Testing Machine

Figure 3.7 Zwick/Roell Tensile Testing
Machine

The Charpy impact energy testing machine is Zwick-Roell RKP 450 which has maximum measurable 450 Joule. The dimensions of impact energy testing were 10x10x55 mm. The samples were held 2 hours at -10°C refrigerator.

3.4) Scanning Electron Microscopy Investigation

The Scanning electron microscopy investigation was done by Jeol JSM-6400 for the coil samples to investigate the morphology of the pearlite-ferrite bands.

CHAPTER 4

RESULTS AND DISCUSSION

The main aim of this project is to reduce the thickness of the pearlite-ferrite bands using soft reduction on API 5L X 65 steel grade and later any effects of soft reduction on mechanical properties are investigated. As mentioned before; the soft reduction depends on the 4 main parameters regarding soft reduction ratio, casting speed, metallurgical length and steel composition. In this experiment; the steel composition was determined according to API 5L PL2 and was tried to be constant. The main alloying elements are titanium, vanadium and niobium. The liqudius temperature of API 5L X 65 is 1518 °C. The super heat was tried to keep between 20 °C and 30 °C.

Table 4.1 Chemical Composition of API X 65 Steel Samples

#	Pouring Temp (°C)	% C	%Mn	%Si	% S	% P	% C Equi.	% Al	% Cu	% N	% Ti	% V	% Nb
1	1552	0,068	1,585	0,165	0,0022	0,0129	0,354	0,0488	0,062	0,0064	0,024	0,040	0,050
2	1542	0,063	1,564	0,163	0,0046	0,0168	0,346	0,0497	0,056	0,0059	0,022	0,038	0,047
3	1547	0,066	1,491	0,161	0,0010	0,0115	0,336	0,0475	0,057	0,0195	0,020	0,036	0,044
4	1546	0,081	1,510	0,158	0,0005	0,0107	0,354	0,0546	0,065	0,0061	0,024	0,036	0,047
5	1545	0,059	1,523	0,132	0,0026	0,0151	0,333	0,0476	0,060	0,0063	0,021	0,035	0,044
6	1549	0,072	1,527	0,187	0,0012	0,0137	0,349	0,0570	0,059	0,0059	0,023	0,034	0,045
7	1546	0,075	1,542	0,168	0,0013	0,0130	0,352	0,0478	0,048	0,0072	0,024	0,036	0,047
8	1545	0,069	1,556	0,154	0,0036	0,0107	0,349	0,0512	0,051	0,0061	0,019	0,035	0,044
9	1545	0,069	1,556	0,154	0,0036	0,0107	0,349	0,0512	0,051	0,0061	0,019	0,035	0,044
10	1549	0,072	1,527	0,187	0,0012	0,0137	0,349	0,0570	0,059	0,0059	0,023	0,034	0,045
11	1546	0,075	1,542	0,168	0,0013	0,0130	0,352	0,0478	0,048	0,0072	0,024	0,036	0,047

The metallurgical length was tried to keep constant using the control of cooling water. To accomplish thin pearlite-ferrite band aim; the effect of casting speed, soft reduction ratio are investigated. According to the variation of casting speed and soft reduction ratio, the optimum values are tried to determine.

Table 4.2 Soft Reduction Index, Soft Reduction Ratio and Casting Speed

#	Casting Temp (°C)	Segregation Index	Soft Reduction Ratio mm/m	Metallurgical Length (mm)	Cast Speed (m/min - avg)	Soft Reduction Zone (mm)	Solidified Wall Thickness of Slab(mm)
1	1552	0	1	23857	1.15	21080-23210	204
2	1542	0	1	23584	1.05	21080-23210	209
3	1547	0	1	24636	1.20	21080-23210	200
4	1546	0	1	24569	1.20	21080-23210	200
5	1545	0	1	24517	1.20	21080-23210	200
6	1549	0.5	1	23590	1.15	21080-23210	204
7	1546	0.5	1.10	23685	1.15	21080-23210	204
8	1545	0.5	-	23857	1.15	Not Applied	204
9	1545	0.5	1.10	23489	1.15	21080-23210	204
10	1549	1	-	23950	1.17	Not Applied	200
11	1546	1	-	24026	1.15	Not Applied	204

4.1) Shell Thickness associated with Heat Transfer Conduction and Convection

To calculate the metallurgical length; the solid thickness should be calculated carefully. There are two ways to calculate the metallurgical length considering solidification constant and heat transfer in the mold. The result of the mathematical calculation can correlate almost with the real thickness when the heat capacity of the water and spray cooling should be calculated carefully. This formulation should be improved according to the mold powder consumption; spray cooling at the exit of the mold; nickel plating of the copper mold [1, 4, 5, 16, 33].

Firstly; the mathematical equation of the solid thickness is following;

$$s = K_s\sqrt{t}$$

(3)

s: The solid (shell) thickness during continuous casting (mm)

K_s: Solidification Constant (mm/min$^{1/2}$)

t: solidification time (min)

Ks; solidification constant can be calculated by the following equation derived from heat transfer analysis under the conditions that temperatures in mould are kept constant when a liquid steel crystallizes;

$$\frac{K_s}{2\sqrt{\alpha}}\exp\left(\frac{K_s{}^2}{4\alpha}\right)\mathrm{erf}(\frac{K_s}{2\sqrt{\alpha}}) = (T_m - T_s)\frac{C_p}{H_f\sqrt{\pi}}$$

(4)

where

α: the thermal diffusivity (m^2/s)

C_p: the specific heat capacity (kJ/kg.K)

H_f: the latent heat (kJ/kg)

T_m: the melting temperature (K)

T_s: the interfacial temperature (K) between a solidifying shell and a mould.

The α thermal diffusivity of low carbon steels (for API 5L X65 steel grade without alloying elements) is 0.682×10^{-5} m^2/sec at 1573°C.

C_p: 0.67 kJ/kg.K

H_f: 272 kJ/kg

According to the literature using the solidification equation; the solidification constant K for low carbon steels without alloying elements is calculated as $22.4\frac{mm}{\sqrt{min}}$.

27

In this research; the solidification constant according to SMS Demag Software program is taken $25.1\frac{mm}{\sqrt{min}}$.

Secondly; regarding heat transfer in the mould the solid thickness can be calculated. Heat equation by convection is following;

$$q = \frac{K\,(T_m - T_s)}{t}$$

(5)

Heat transfer equation at the solidified steel/mould interface is following;

$$q = h(T_s - T_w)$$ (6)

Combining the equation 3 and equation 4;

$$q = T_m - T_s$$ (7)

$$\frac{q}{h} = T_s - T_o$$

(8)

$$q\left(\frac{t}{K} + \frac{1}{h}\right) = T_m - T_o$$

(9)

The first heat equation is following;

$$q_1 = \frac{T_m - T_o}{(\frac{t}{K} + \frac{1}{h})}$$

(10)

The total heat evolved because of the latent heat and superheat is following;

$$q_2 = \rho_s(\Delta H + C_p\Delta T)\frac{dt}{dQ}$$

(11)

28

The two heat equations should be equal to each other;

$$q_1 = q_2$$

(12)

Equating q_1 and q_2 equations;

$$\frac{T_m - T_o}{\left(\frac{t}{K} + \frac{1}{h}\right)} = \rho_s(\Delta H + C_p \Delta T)\frac{dt}{dQ}$$

(13)

Where L= full thickness and t= solidifying thickness t=L/2

$$L_{eff} = \Delta H + C_p \Delta T$$

(14)

Calculating the equations yields a general equation for thermal boundary thickness equation for the condition; t=0 at θ =0 and t=t at $\theta = \theta$ r

$$\int_0^Q \left(\frac{T_m - T_0}{\rho_s L_{eff}}\right) dQ = \int_0^t \left(\frac{t}{K} + \frac{1}{h}\right) dt$$

(15)

$$\left(\frac{T_m - T_0}{\rho_s L_{eff}}\right) Q_r = (\frac{t^2}{2K} + \frac{1}{h})$$

(16)

Obtaining the positive root of this equation; the boundary layer thickness can be calculated associated with heat transfer.

$$t^2 + \frac{2Kt}{h} - \frac{2K(T_m - T_0)Q_r}{\rho_s L_{eff}} = 0$$

(17)

The results can be concluded from the following equation;

$$t_{1,2} = \frac{-\frac{2K}{h} \pm \sqrt{(\frac{2K}{h})^2 - 4(-\frac{2K(T_m - T_o)Q_r}{\rho_s L_{eff}})}}{2}$$

(18)

29

h= gap heat transfer coefficient h= 400 W/m^2K

K=thermal conductivity of API X 65 Steel grade K=51 W/m^2K at 25 °C.

Q= Heat Flow Rate Q = 477400 W (for the mould dimensions 1500*900 mm (disregarding nickel plating)

The steel casting dimensions are 1500*230 mm at the exit of the mould.

T_m = Melting Temperature T_m= 1518 °C for API X 65 steel grade

T_o= Temperature at the exit of the copper mould T_o =1100 °C.

C_p: 0.67 kJ/kg.K for API X 65 steel grade

H_f: 272 kJ/kg for API X 65 steel grade

ρ_s = 7,8 gr/ cm^3

According to above the calculations the thickness of the solidified API X65 grade steel at the exit of the mould;

Thickness=15.92 mm

When the heat conduction in the mould is considered, the following calculation should be done for any steel grade;

➢ The mold length is 800 mm.

➢ The pouring temperature is 1823 K.

➢ The liquidus temperature is 1793 K.

➢ The wide of steel slab is 1500 mm.

➢ The thickness of steel slab is 225 mm.

➢ The increase of the cooling water is 7 K.

➢ The temperature of the cooling water is 297 K.

➢ The surface temperature of the copper mold is 573 K.

➢ Latent heat of fusion is 2.67 x 10^5 J kg^{-1},

➢ Solid density is 7690 kg m^{-3},

➢ Solid heat capacity = 670 J kg^{-1} K^{-1},

➢ Liquid heat capacity = 596 J kg^{-1} K^{-1},

➢ Solid thermal conductivity = 60 W m^{-1} K^{-1}

➢ The flow rate of water is 2800 kg/min.

➢ The specific heat of water is 4184 J Kg^{-1} K^{-1}

➢ The casting speed is 0.016 mm/sec (1 m/min).

➢ Heat transfer Coefficient Transfer (h) is 2000 W/m^2K

$$H_{f'} = H_{f'} + C_p(T_p + T_m)$$

(19)

$$H_{f'} = 2.67 * 10^5 \frac{J}{kg} + 596 \frac{J}{kgK} * 40\,K = 243160 \frac{J}{kg}$$

(20)

$$\frac{H_f}{C_p(T_m - T_0)} = \frac{243160}{670 * (1793 - 573)} = 0.297$$

(21)

$$\frac{h^2 y}{uk\rho C_p} = \frac{2000^2 * 0{,}80}{7690 * 60 * 670 * 0.016} = 0.64$$

(22)
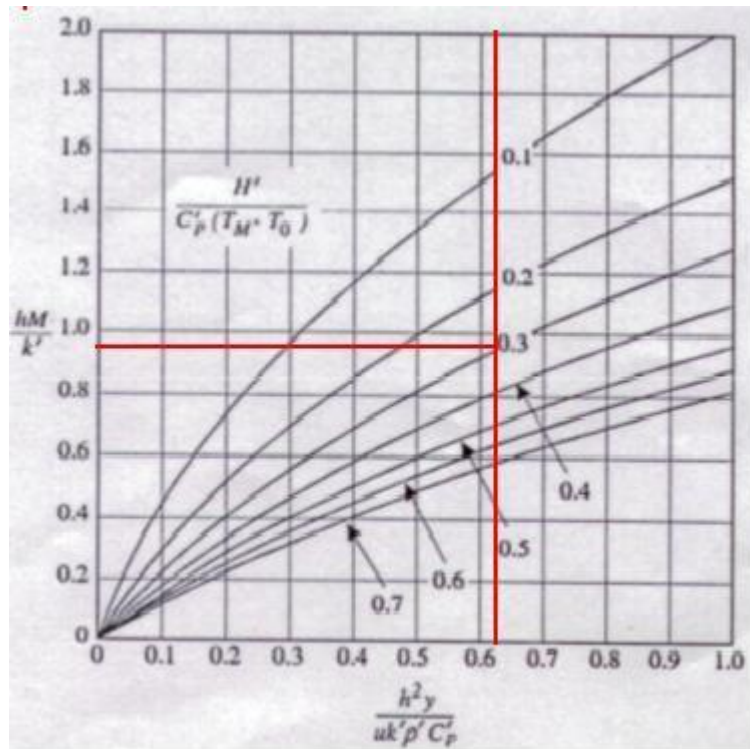
Figure 4.1: Thickness solidified, M, versus distance down the mold [37].

$$\frac{hM}{K'} = 0.977$$

31

$$\frac{2000M}{60} = 0.977$$

Solidified Thickness of Slab at the exit of the mold

$$M = 0.032 \, m = 32 \, mm$$
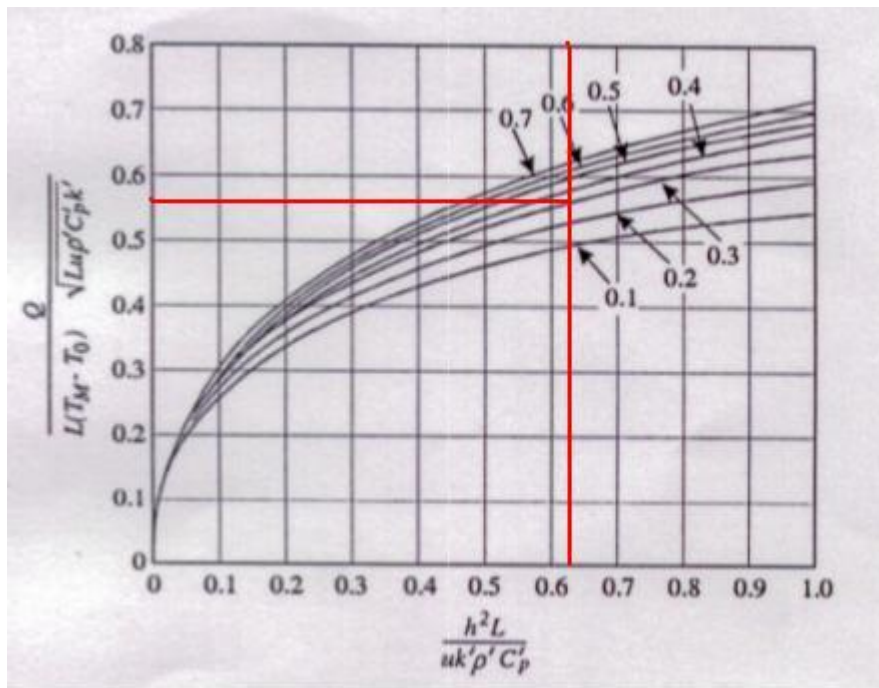
Figure 4.2: Rate of heat removal by mold cooling water versus mold length L. Numbers on the curves are the same [37].

From the figure 4.2;

$$\frac{Q}{L(T_m - T_0\sqrt{Lu\rho C_p k}} \cong 0.57$$

$$Q = (0.55)(0.80)(1793 - 573)\sqrt{(0.80)(0.016)(7690)(670)(60)} = 0.57$$

<div align="right">(27)</div>

$$Q = 1.06*10^6\,\text{W}$$

<div align="right">(28)</div>

$$\text{Flow Rate} = 1.06*10^6 \frac{J}{S}\frac{KgK}{4184\ J\ 7\ K} = 36.19 \text{ kg/sec.}$$

<div align="right">(29)</div>

$$\text{Flow Rate} = 2171 \text{ kg/min.}$$

<div align="right">(30)</div>

The minimum and actual flow rate (constant during casting) considering SMS Demag software program = 2400 kg/min and 2800 kg/min; respectively.
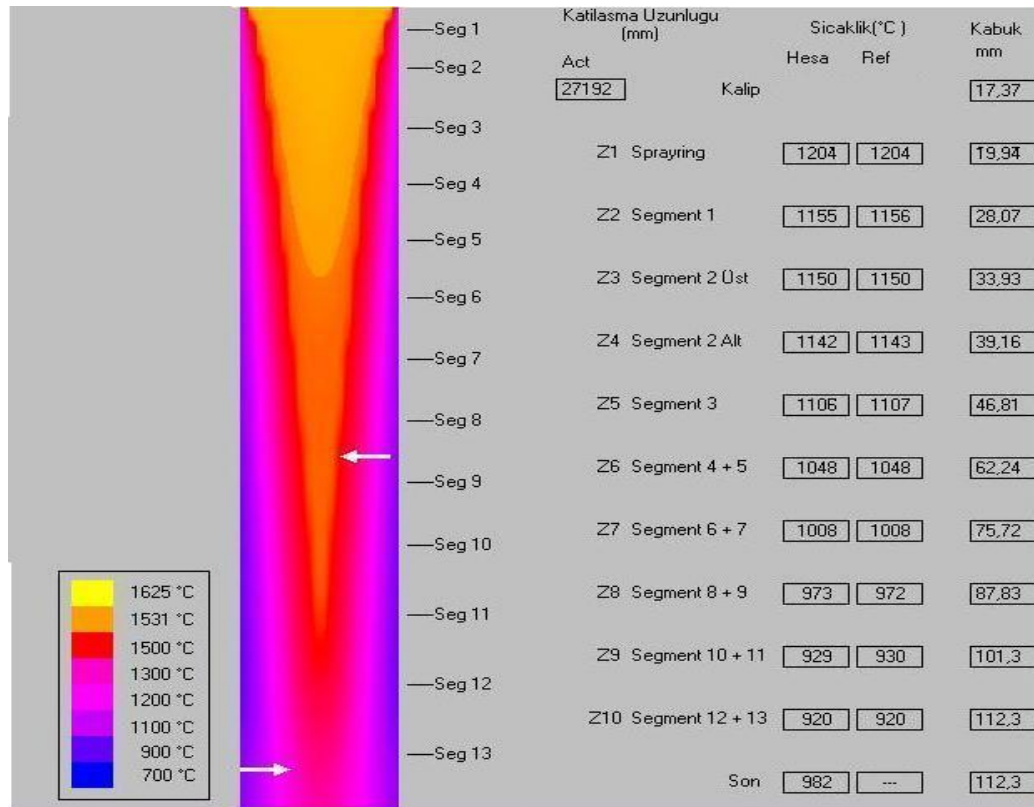
Figure 4.3: SMS Demag the actual metallurgical length calculation at the casting speed 1.20 m/min. for low carbon steel. [38]
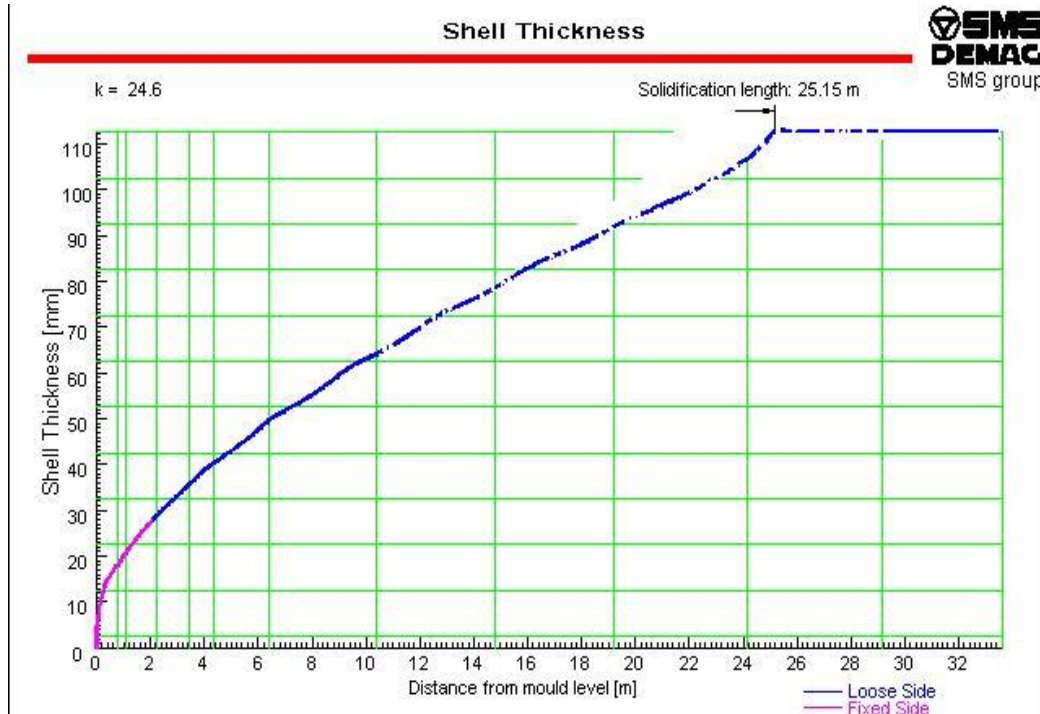
Figure 4.4: SMS Demag the actual metallurgical length calculation. [38]

In this research the SMS Demag solidification program was used to calculate the metallurgical length and also according to literature calculations; the SMS Demag program is confirmed.

Considering required mold cooling water; the solidified thickness of slab in the mold was re-calculated using convection model to verify the heat transfer coefficient.

Following data was taken into consideration for API X 65 steel grade;

➢ The casting speed was 1.20 m/min.

➢ Thermal Conductivity is 51 W/m^{2}K.

➢ The liquidus temperature is 1793 K.

➢ The density is 7850 kg/m^3.

➢ The mold cooling water is 303.6 K.

➢ The temperature increase of the mold cooling water is 4.5 K.

➢ Flow Rate is 3900 Kg/min=65 kg/sec.

$$Q = \text{Flow Rate} * 4184 \text{ J} * 4.5 \text{ K}.$$

(31)

$$Q = 1223820 \text{ W}$$

(32)

34

$$\frac{Q}{L(T_m - T_0)\sqrt{Lu\rho'C_p'K'}}$$

$$= \frac{1223820}{0.675 * (1793 - 303.6)\sqrt{0.675 * 0.02 * 7850 * 670 * 51}} = 0.64$$

(33)
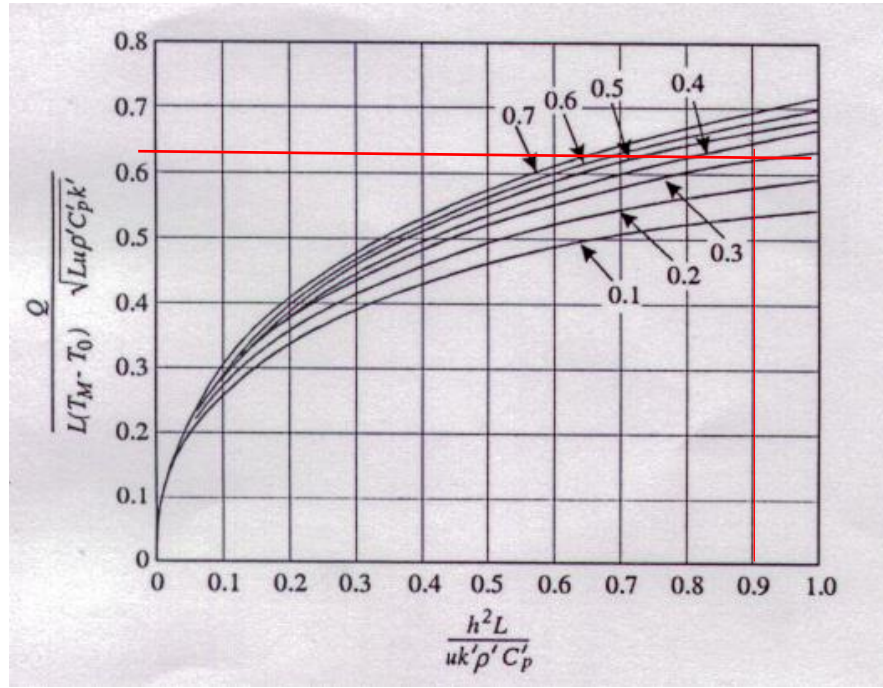
Figure 4.5: Rate of heat removal by mold cooling water versus mold length L regarding the required mold cooling water 3900 kg/min. Numbers on the curves are the same. [37]

$$\frac{h^2 y}{uk'\rho'C_p'} = \frac{h^2 0.675}{0.02 * 7850 * 670 * 51} - 0.936$$

(34)

The heat transfer coefficient regarding actual cooling water 3900 Kg/min is

$$h = 2727 \text{ W/ m}^2\text{K}$$

(35)

35
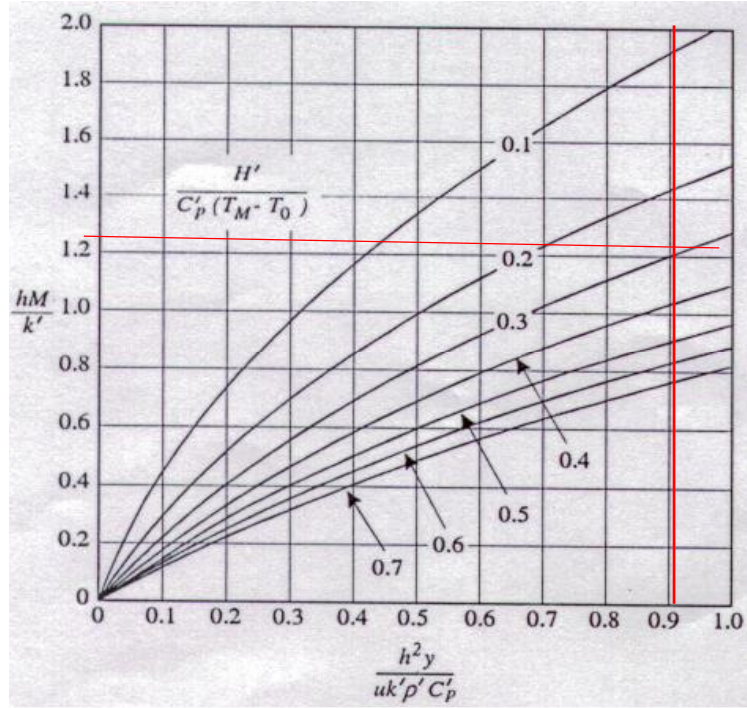
Figure 4.6: Thickness solidified, M, versus distance down the mold [37].

$$\frac{h^2 y}{uk'\rho'C'_p} = \frac{2727^2 * 0.675}{0.02 * 7850 * 670 * 51} = 0.936$$

(36)

$$\frac{hM}{k'} = 1{,}21$$

(37)

$$M = 0.022 \text{ m} = 22 \text{ mm.}$$

(38)

The calculated solidified thickness at the exit of the mold regarding the actual mold cooling water and the temperature increase of the mold cooling water is 22 mm. The SMS Demag program calculates around 17 mm. The difference is 5 mm which can be caused by several reasons such as instant temperature increase of the cooling water or mold powder gets thinner at that instant because SMS Demag program is dynamic program which gets the data instantly.

4.2) Macro and Micro Structure Investigation Results

At the beginning; 11 samples were classified considering the casting cavities according to the Mannesmann Index from "0" good surface to "1" bad cavity quality. To be more specific; "0" index means that there is no casting cavities and minimum segregation. On the other hand; "1" index means that there are casting cavities inside the slab and more segregation is observed. Secondly; after hot rolling process the samples were taken from the coils and the thickness of pearlite-ferrite bands were measured and listed. In general view; the macro-figures correlates with the micro-figures. In other words; the thickness of pearlite-ferrite band becomes thicker from "0" index to "1" index. Regarding macro figures; sample 1, 2, 3, 4, 5 are "0" segregation index, sample 6, 7, 8, 9 are "0.5" segregation index and sample 10, 11 are "1" segregation index. Comparing the macro figures; the best results belong to sample 2 and 3; however, the worst result belongs to sample 10. Sample 2 and 3 did not have any sign of casting cavity on the surface regarding the 2 different sides. On the other hand; Sample 10 had serious casting cavities on both sides. Especially; the parallel direction side to casting of sample 10 had wider casting cavities than the perpendicular direction to casting. The main difference between the "0.5" index and "1" index is the continuity of the casting cavities. For instance; comparing the sample 8 with sample 10; the wide of casting cavity is almost same for both sample. However; the casting cavities of sample 8 are not continuous.

Figure 4.7 Macro Sample 1 Side 3
Soft Reduction Ratio is 1 mm/m.
Casting Speed is 1.15 m/min.
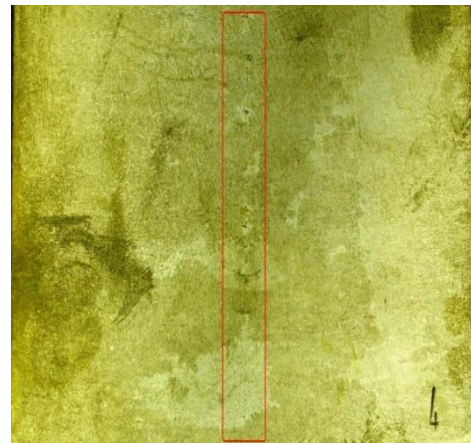
Figure 4.8 Macro Sample 1 Side 4
Soft Reduction Ratio is 1 mm/m.
Casting Speed is 1.15 m/min.

Figure 4.9 Macro Sample 3 Side 3
Soft Reduction Ratio is 1 mm/m
Casting Speed is 1.20 m/min.

Figure 4.10 Macro Sample 3 Side 4
Soft Reduction Ratio is 1 mm/m.
Casting Speed is 1.20 m/min.

Figure 4.11 Macro Sample 6 Side 3
Soft Reduction Ratio is 1 mm/m.
Casting Speed is 1.15 m/min.

Figure 4.12 Macro Sample 6 Side 4
Soft Reduction Ratio is 1 mm/m.
Casting Speed is 1.15 m/min.
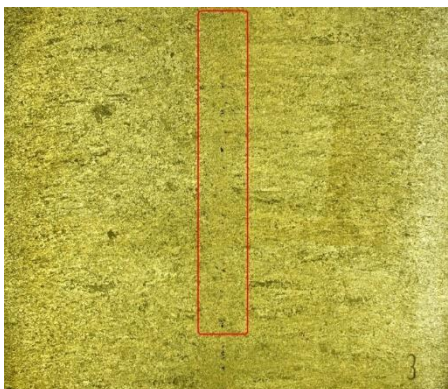
Figure 4.13 Macro Sample 7 Side 3
Soft Reduction Ratio is 1.10 mm/m.
Casting Speed is 1.15 m/min.
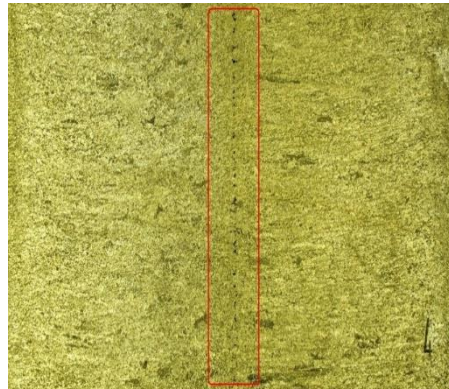
Figure 4.14 Macro Sample 7 Side 4
Soft Reduction Ratio is 1.10 mm/m.
Casting Speed is 1.15 m/min.

Figure 4.15 Macro Sample 8 Side 3
Soft Reduction is not applied.
Casting Speed is 1.15 m/min.

Figure 4.16 Macro Sample 8 Side 4
Soft Reduction is not applied.
Casting Speed is 1.15 m/min.
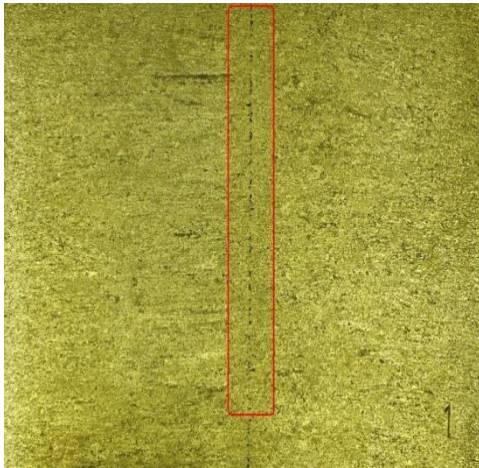
Figure 4.17 Macro Sample 11 Side 3
Soft Reduction is not applied.
Casting Speed is 1.15 m/min.
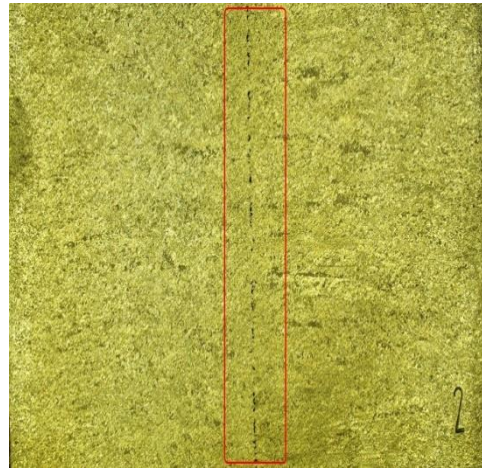
Figure 4.18 Macro Sample 11 Side 4
Soft Reduction is not applied.
Casting Speed is 1.15 m/min.
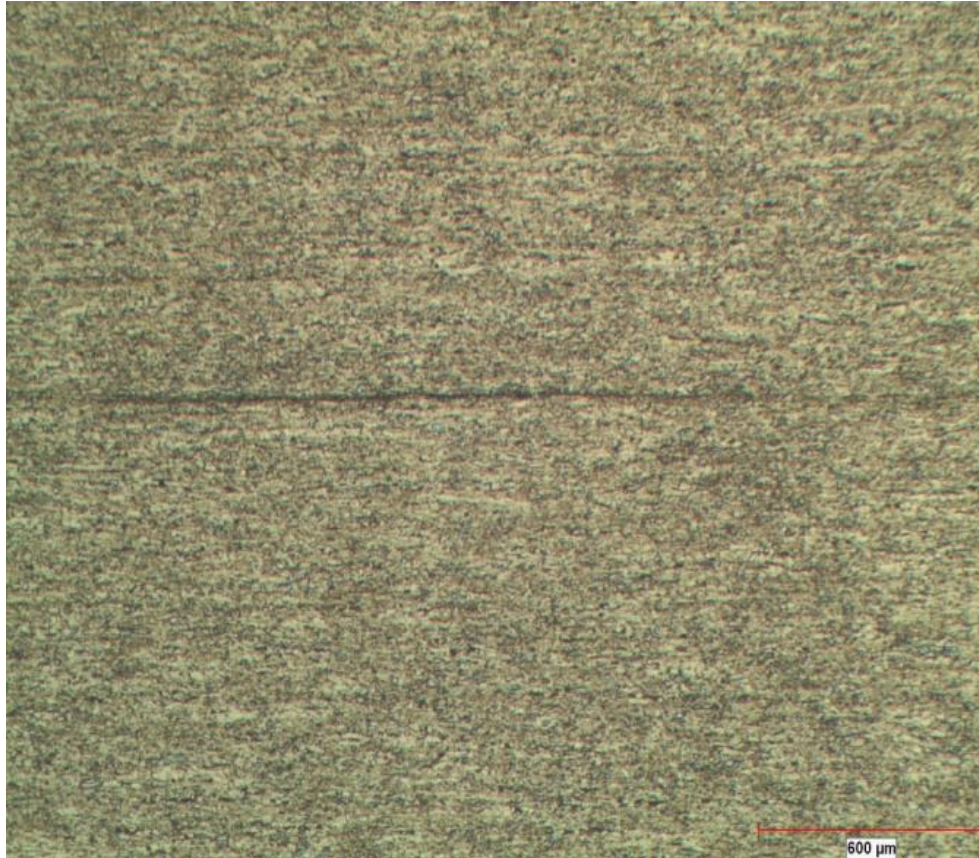
Figure 4.19 X25 Micro Structure of Sample 1 Soft Reduction Ratio is 1 mm/m. Casting Speed is 1.15 m/min.
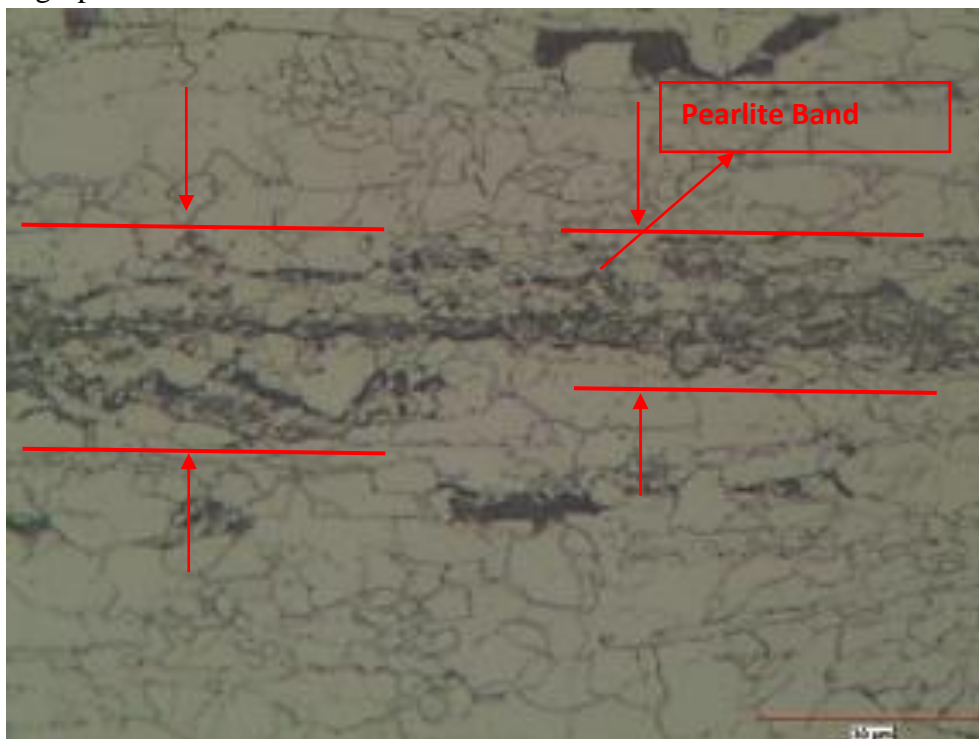
Figure 4.20 X500 Micro Structure of Sample 1 Soft Reduction Ratio is 1 mm/m. Casting Speed is 1.15 m/min. The arrows show where the thickness is measured.

Figure 4.21 X25 Micro Structure of Sample 2 Soft Reduction Ratio is 1 mm/m. Casting Speed is 1.05 m/min.

Figure 4.22 X500 Micro Structure of Sample 2 Soft Reduction Ratio is 1 mm/m. Casting Speed is 1.05 m/min. The arrows show where the thickness is measured.
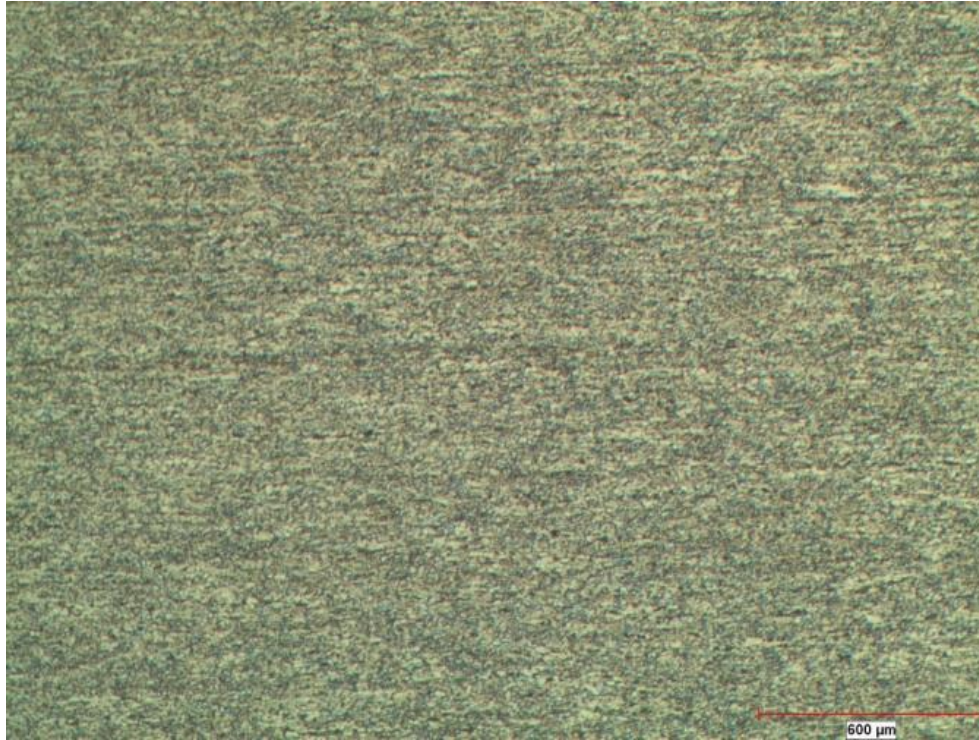
Figure 4.23 X25 Micro Structure of Sample 3 Soft Reduction Ratio is 1 mm/m. Casting Speed is 1.20 m/min.

Pearlite Band
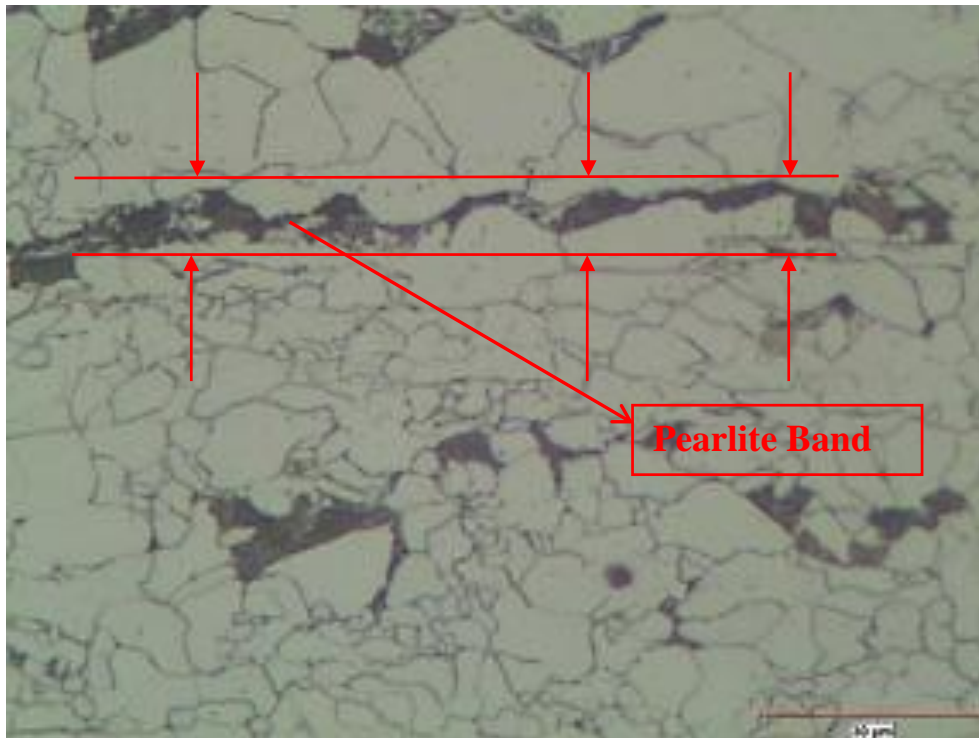
Figure 4.24 X500 Micro Structure of Sample 3 Soft Reduction Ratio is 1 mm/m. Casting Speed is 1.20 m/min. The arrows show where the thickness is measured.

When micro and macro structure figures are compared together; the best result belongs to the sample 3. There is very thin pearlite-ferrite band barely seen in X25 micro figure of sample 3 supporting to the macro figures. The thickness of this band varies from 9.37 μm to 13.12 μm. It can be said that the pearlite-bands were dispersed to centre of coil. It is worth to mention that the soft reduction ratio was 1 mm/m. and the casting speed was 1.20 m/ min. Supporting the result of sample 3; when the same soft reduction ratio and casting speed was applied to sample 5; and the micro structure figures of sample 5 are investigated; several thin pearlite-ferrite bands can be seen. The thicknesses of these bands change from 9.35 to 15.10 μm. However; the pearlite-ferrite band of sample 3 in X25 micro figure can barely be seen. The position of soft reduction zone was not changed. The only difference between these sample 3 and 5 is metallurgical length. The metallurgical lengths of sample 3 and sample 5 are 24636 mm and 24517 mm, respectively. To be clearer, the metallurgical length of sample 3 was longer than the sample 5. The difference; which is 116 mm, can be resulted from the cooling water. To conclude this comparison; the longer metallurgical length could make thinner pearlite-ferrite band at same casting speed and soft reduction ratio.

Figure 4.25 X25 Micro Structure of Sample 4 Soft Reduction Ratio is 1 mm/m. Casting Speed is 1.20 m/min.

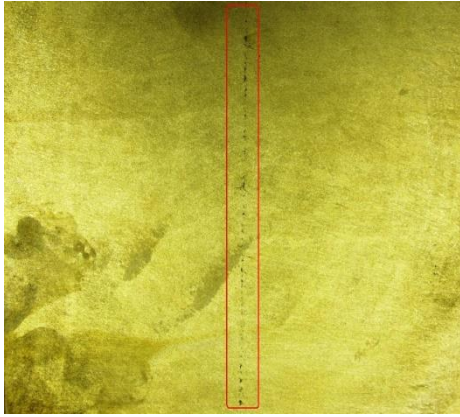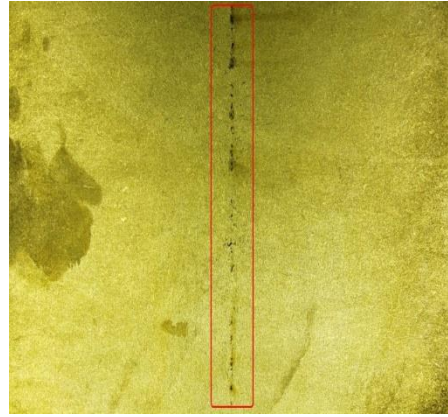**Figure 4.26** X500 Micro Structure of Sample 4 Soft Reduction Ratio is 1 mm/m. Casting Speed is 1.20 m/min. The arrows show where the thickness is measured.

Figure 4.27 X25 Micro Structure of Sample 5 Soft Reduction Ratio is 1 mm/m. Casting Speed is 1.20 m/min.

Figure 4.28 X500 Micro Structure of Sample 5 Soft Reduction Ratio is 1 mm/m. Casting Speed is 1.20 m/min. The arrows show where the thickness is measured.

Figure 4.29 X25 Micro Structure of Sample 6 Soft Reduction Ratio is 1 mm/m. Casting Speed is 1.15 m/min.

Figure 4.30 X500 Micro Structure of Sample 6 Soft Reduction Ratio is 1 mm/m. Casting Speed is 1.15 m/min. The arrows show where the thickness is measured.
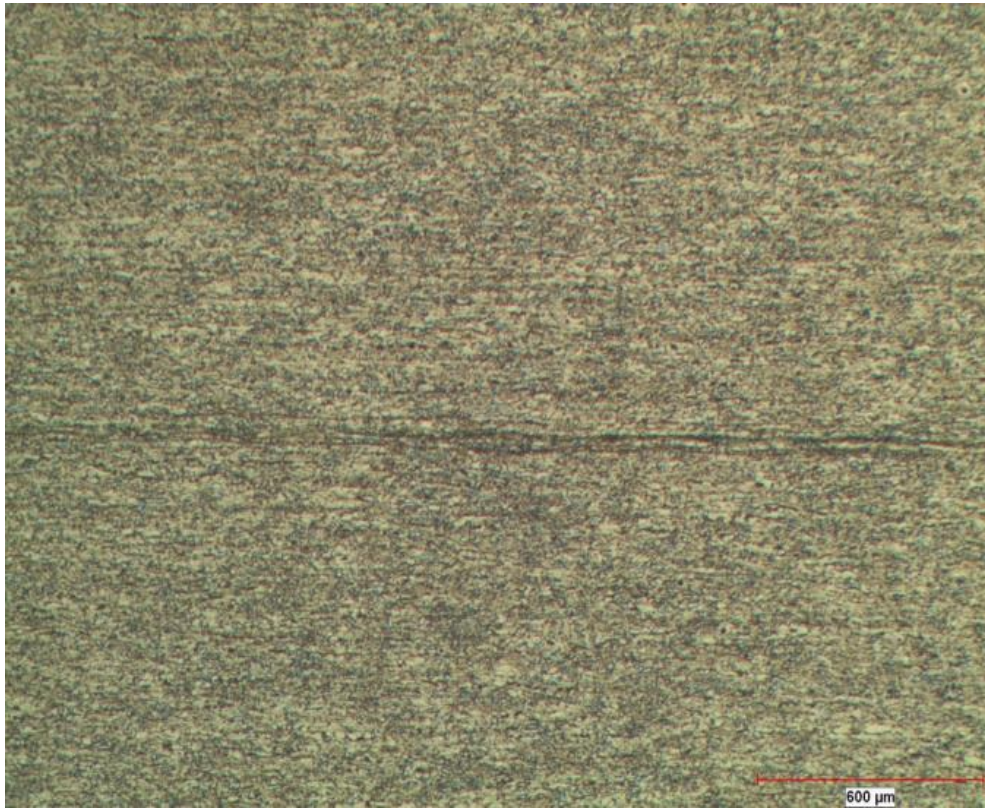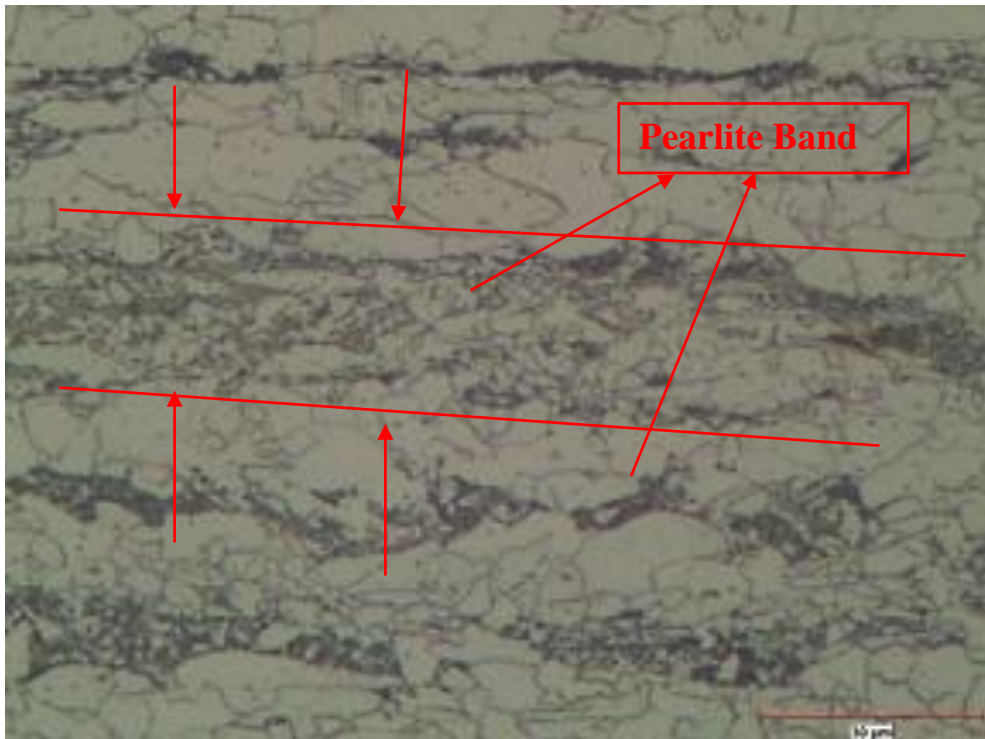

Figure 4.31 X25 Micro Structure of Sample 7 Soft Reduction Ratio is 1.10 mm/m. Casting Speed is 1.15 m/min.

Figure 4.32 X500 Micro Structure of Sample 7 Soft Reduction Ratio is 1.10 mm/m. Casting Speed is 1.15 m/min. The arrows show where the thickness is measured.

Sample 7 is "0.5" segregation index. The soft reduction ratio was 1.10 mm/m. The casting speed was 1.15 m/min. When the X25 micro-structure figure of sample 7 is examined; it can be seen that there is one pearlite-ferrite band. The thickness of this band changes from 10 μm to 38 μm. The pearlite-ferrite band thickness of sample 7 is thicker than sample 3; however, thinner than sample 11. In this sample the soft reduction ratio was increased at the casting speed 1.15 m/min. by this way; the pearlite band thickness is decreased comparing with sample 1. This fact supports the idea that the soft reduction makes the pearlite-ferrite band thinner.

Figure 4.33 X25 Micro Structure of Sample 8 Soft Reduction Ratio is not applied. Casting Speed is 1.15 m/min.

Pearlite Band

Figure 4.34 X500 Micro Structure of Sample 8 Soft Reduction Ratio is not applied. Casting Speed is 1.15 m/min. The arrows show where the thickness is measured.

Sample 8 is "0.5" segregation index. The casting speed is 1.15 m/min. The soft reduction is not applied. Although the macro figure seems relatively good, the micro structure figure shows that the pearlite-ferrite band is thick. The total thickness is 88 µm. This proves that the soft reduction makes the pearlite-ferrite band thin.

Figure 4.35 X25 Micro Structure of Sample 9 Soft Reduction Ratio is 1.20 mm/m. Casting Speed is 1.15 m/min.
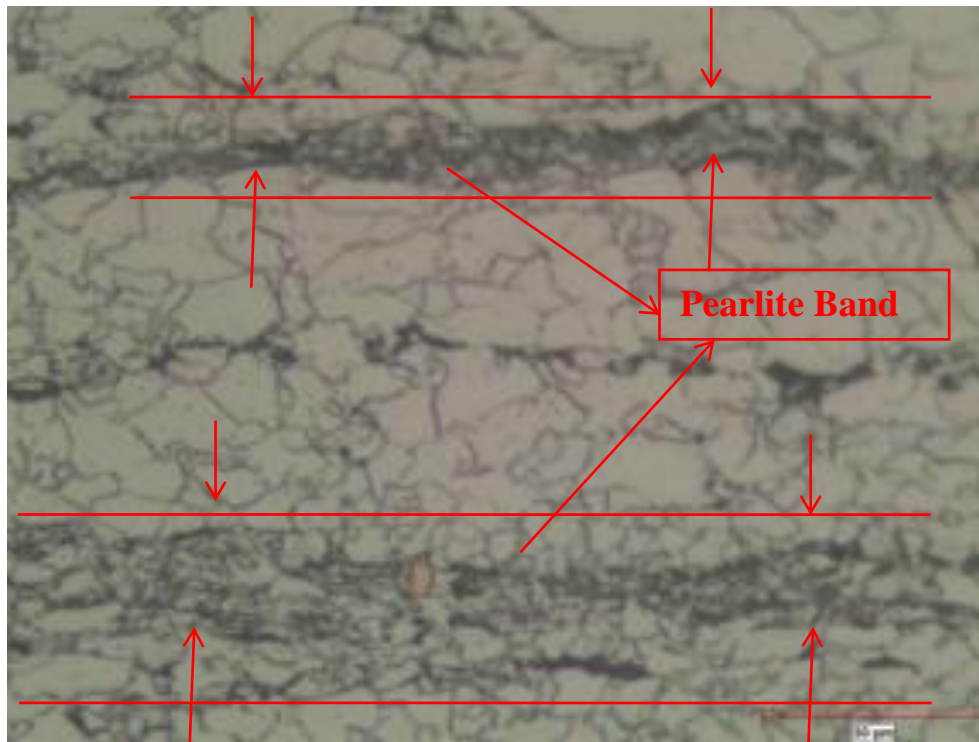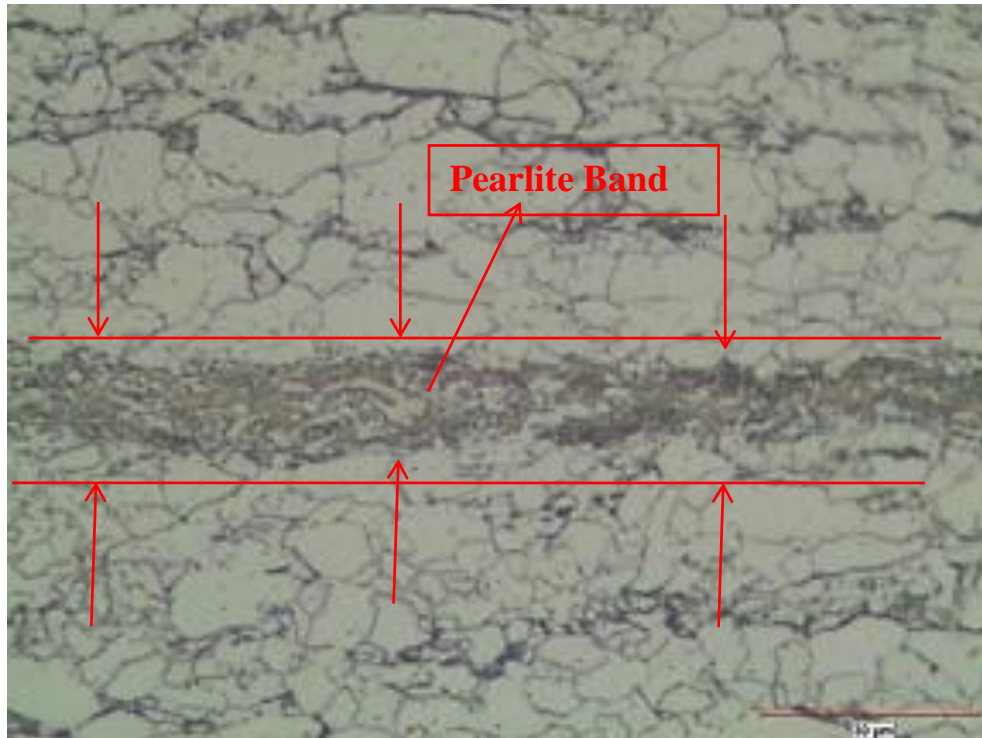
Figure 4.36 X500 Micro Structure of Sample 9 Soft Reduction Ratio is 1.20 mm/m. Casting Speed is 1.15 m/min. The arrows show where the thickness is measured.

Sample 9 is also "0.5" segregation index. The soft reduction ratio was 1.20 mm/m. The casting speed was 1.15 m/min. The X25 micro structure figure of sample 9 shows that there is thin pearlite band in the centre. The thickness of this band changes from 8 to 15 μm. Comparing the sample 3 and sample 9; the effect of solidified shell wall thickness on the soft reduction during continuous casting can be clearly seen. The morphology of sample 9 pearlite-ferrite band is more dispersed comparing to sample 3.

The reason can be explained by the solid wall thickness of the slab. The actual thickness of the sample 9 between the soft reduction zones during continuous casting was 227.7 mm. The solid wall thickness of the sample 3 and 9 during continuous casting was 200 and 204 mm; respectively. The liquid thickness of sample 3 and 9 is 27.7 mm and 23.7 mm; respectively. To illustrate the situation; because of the applied force using the soft reduction; pressurized liquid steel in front of growing dendrite results in either breaking of dendrite or penetrate to the space between the dendrites. The dendrite strength of sample 9 is higher than the strength of sample 3 during continuous casting. In addition; the alloying rich liquid of sample

3 had more time to penetrate to the casting cavities than sample 9. Therefore; the sample 3 has thinner pearlite-ferrite band than sample 9. The dispersed pearlite-ferrite band of sample 9 proves this claim.

Figure 4.37 X25 Micro Structure of Sample 10 Soft Reduction is not applied. Casting Speed is 1.17 m/min.

Figure 4.38 X500 Micro Structure of Sample 10 Soft Reduction is not applied. Casting Speed is 1.17 m/min. The arrows show where the thickness is measured.
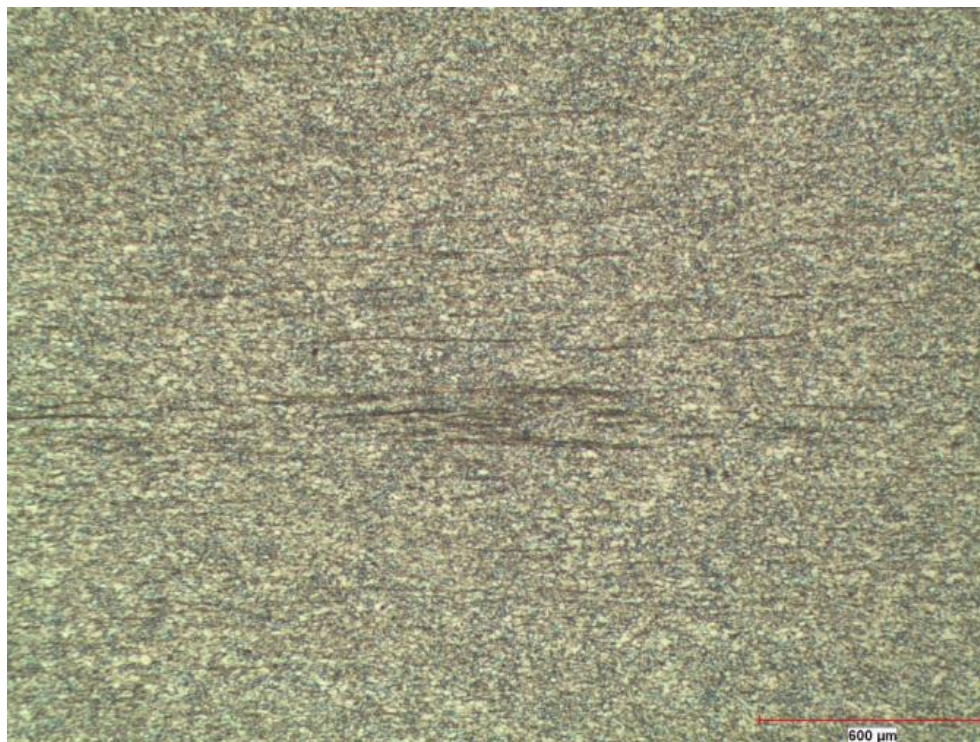
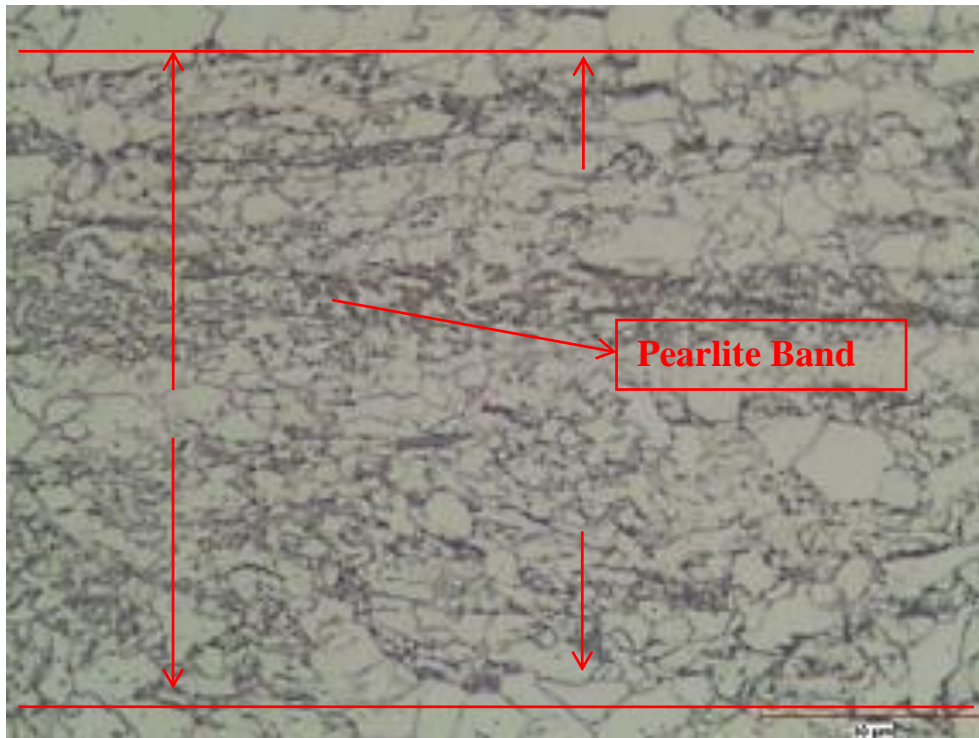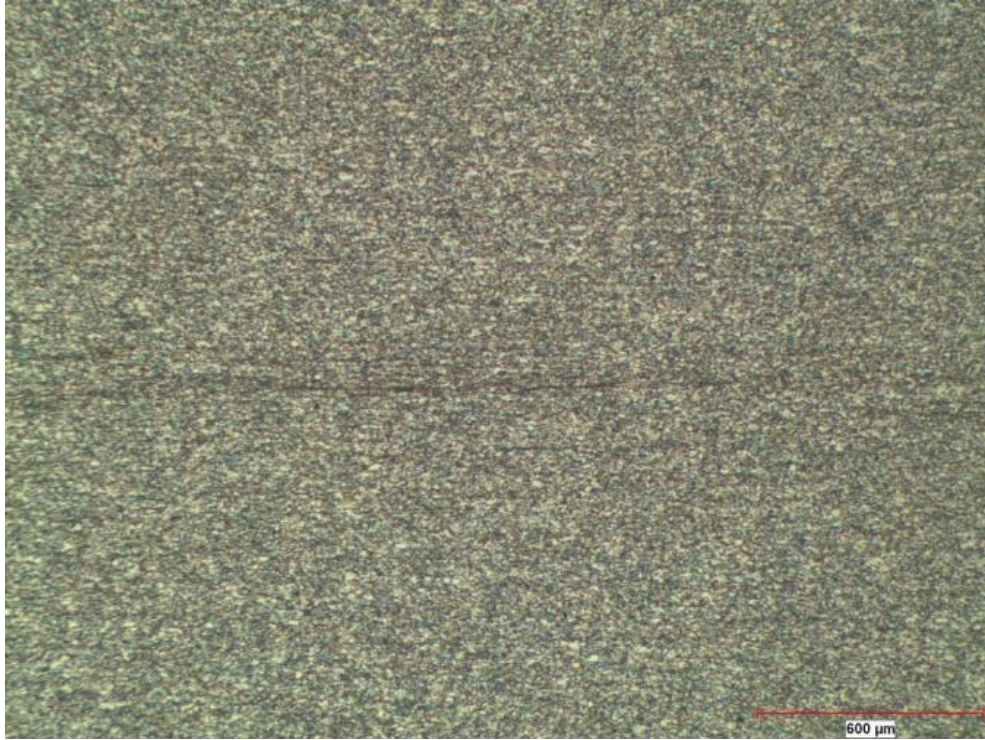**Figure 4.39** X25 Micro Structure of Sample 11 Soft Reduction is not applied. Casting Speed is 1.15 m/min.

Pearlite Band
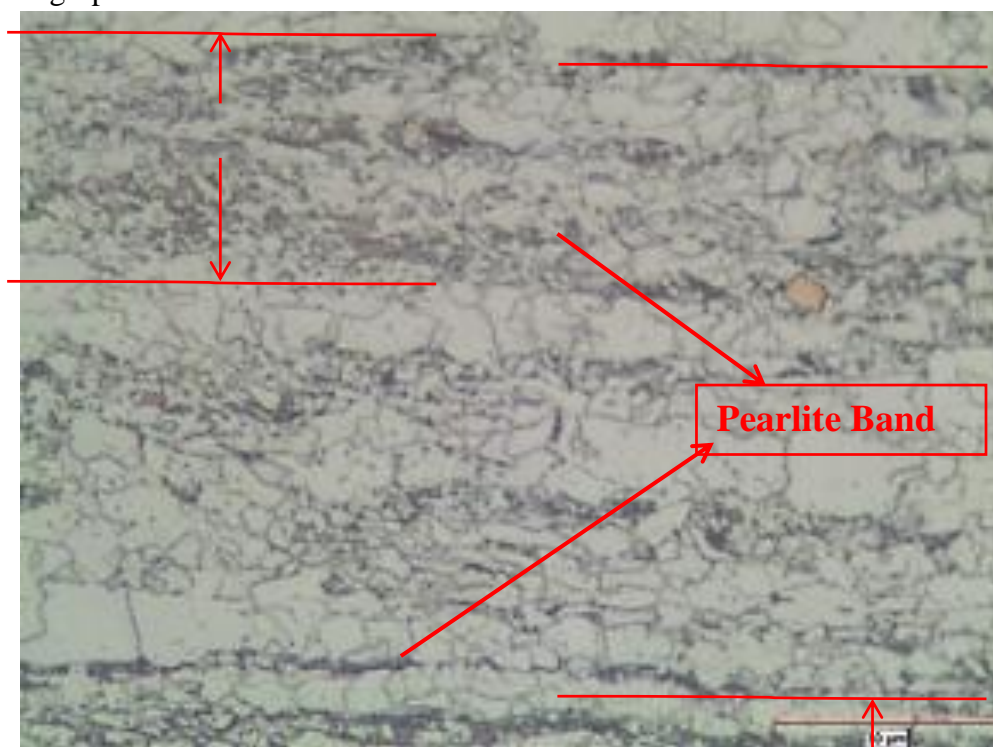
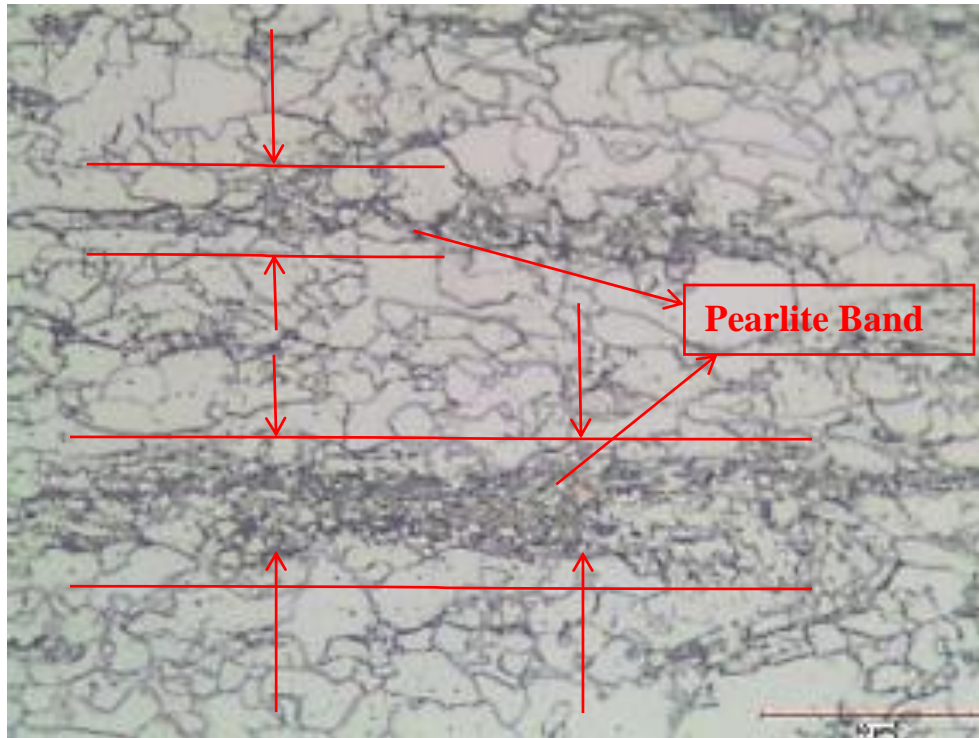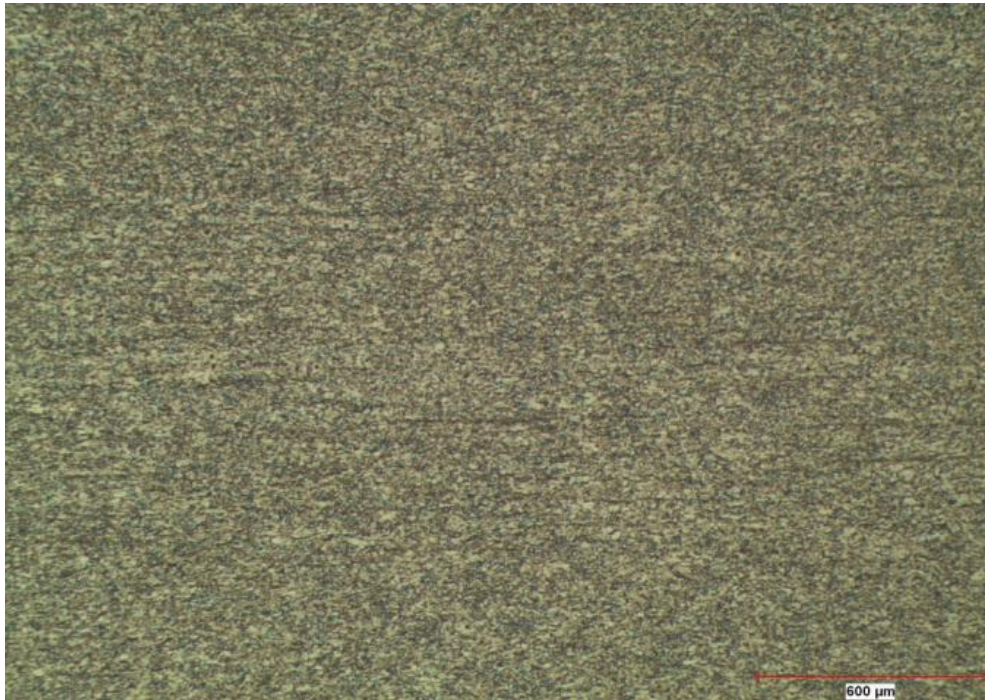**Figure 4.40** X500 Micro Structure of Sample 11 Soft Reduction is not applied. Casting Speed is 1.15 m/min. The arrows show where the thickness is measured.
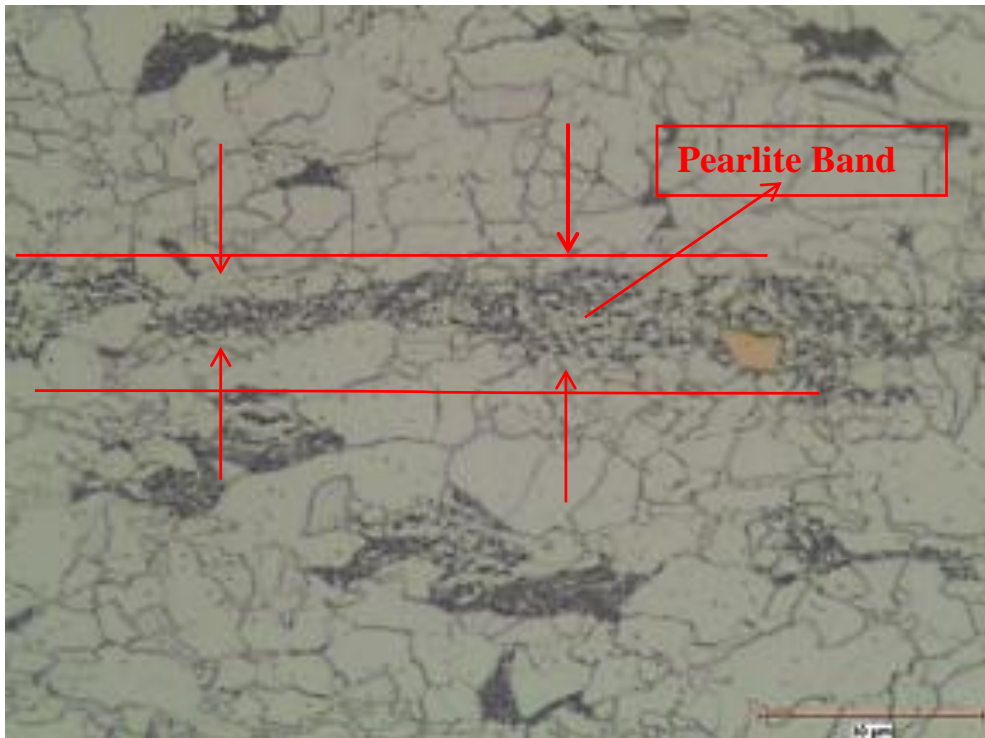
Comparing the only micro-structure figures of coils; the worst result belongs to sample 11. The pearlite-ferrite bands can be seen at X25 micro structure figure of sample 11. In addition there are several pearlite-ferrite bands in the X25 micro structure figure of sample 11. The thickness of these bands varies from 31 µm and 94 µm. The main differences of sample 11 from other samples are more than one band in the centre line and the thicker pearlite-ferrite bands. The soft reduction was not applied to this sample 11. The casting speed was 1.15 m/min. When the macro-structure figures of sample 11 and sample 10 were compared; the sample 10 had more casting cavities. On the other hand; the pearlite-thickness of sample 11 are thicker than sample 10. The reason is probably that the sample 10 was cut from the slab which soft reduction was stopped in the middle slab. In other words; the effect of soft reduction was continuing on the slab during casting. The sample 11 was taken from the slab 1 hour later after soft reduction was stopped. Comparing the sample 3 and sample 11; it can be seen clearly that the thickness of pearlite-ferrite band of sample 3 was thinner than sample 11. In addition; the pearlite-ferrite band of sample 11 was dispersed in wide area.

The grain sizes of all samples were measured using X200 micro figures according to the ASTM E112-96 standard using the Clemex Professional Edition Software Program and listed in Table 4.3. It should be pointed out that the same heat treatment method regarding 1200ºC annealing and hot rolling was applied to the all samples. Comparing all sample grain sizes; it can be concluded that the soft reduction does not have any effect on the grain sizes.

Table 4.3 Segregation Index "0" Samples. Grain Size and Pearlite-Ferrite Thickness. The grain sizes are measured according to the ASTM E112-96 standard.

#	Grain Size (µm)	Pearlite-Ferrite Thickness (µm)					
		1	2	3	4	5	Average
1	11	17	19	21	23	28	22
2	11	19	22	23	24	24	22
3	11	8	9	11	12	13	11
4	11	7	7	13	13	15	11
5	11	9	12	13	14	15	13
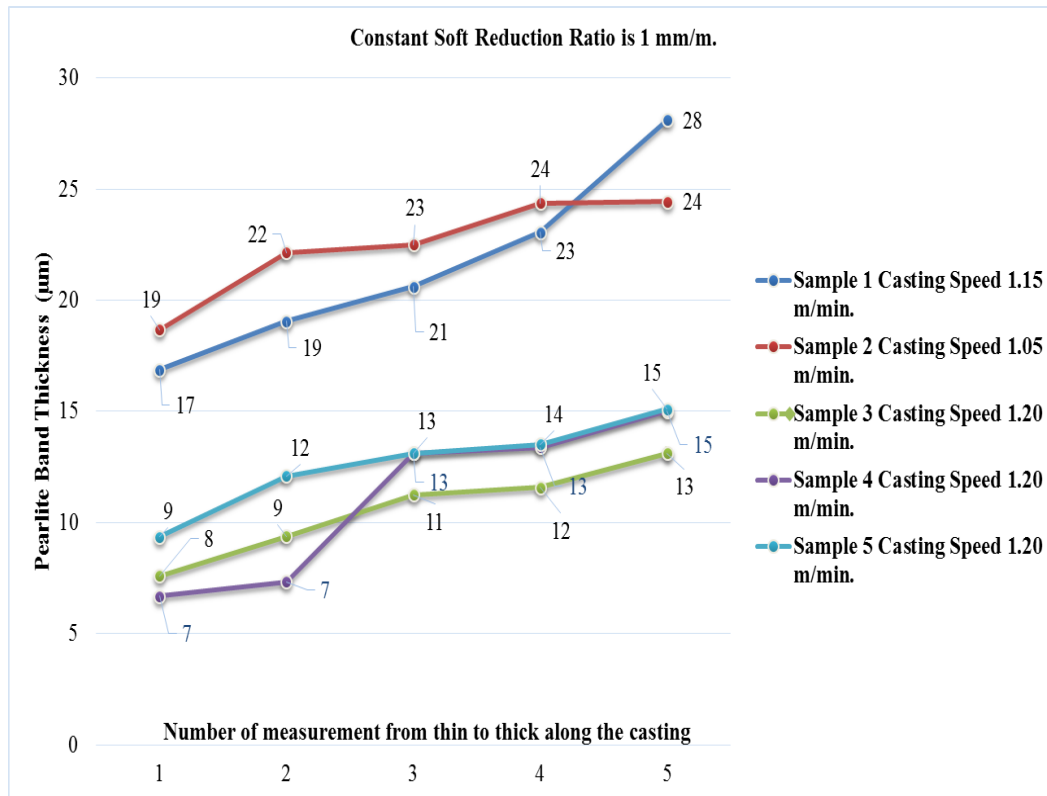
Figure 4.41 Segregation Index "0" Samples. The thickness variation is small along the pearlite band. Soft Reduction Ratio is same for these samples and 1.00 mm/m. Casting Speeds are written on the figure.

Table 4.4 Segregation Index "0.5" Samples. Grain Size and Pearlite-Ferrite Thickness. The grain sizes are measured according to the ASTM E112-96 standard.

#	Grain Size (µm)	Pearlite-Ferrite Thickness (µm)					
		1	2	3	4	5	Average
6	11	17	24	26	70	74	42
7	11	10	12	14	24	38	20
9	11	8	9	9	13	15	11
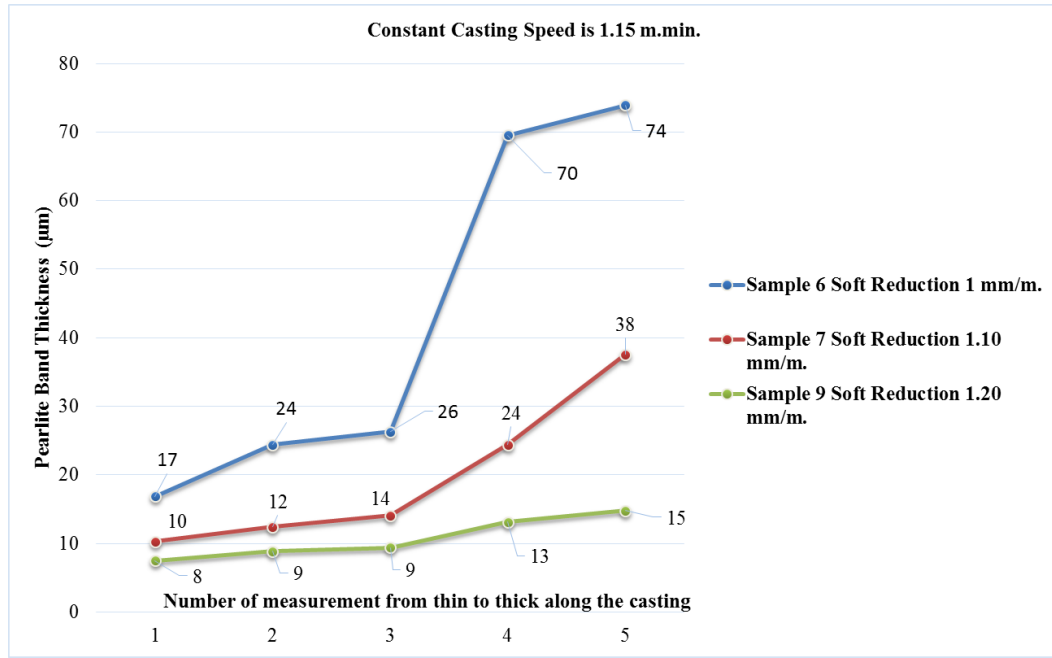
Figure 4.42 Segregation Index "0.5" Samples. The thickness variation of segregation index "0.5" samples along the pearlite band are larger than segregation index "0". The casting speed is 1.15 m/min.

Table 4.5 Soft Reduction is not applied. Grain Size and Pearlite-Ferrite Thickness. The grain sizes are measured according to the ASTM E112-96 standard. Soft reduction is applied on the half of the sample 10 and then de-activated because of sticking alarm.

#	Grain Size (µm)	Pearlite-Ferrite Thickness (µm)					
		1	**2**	**3**	**4**	**5**	**Average**
8	11	69	73	81	87	88	80
10	11	11	15	17	17	20	16
11	11	31	50	89	93	94	72
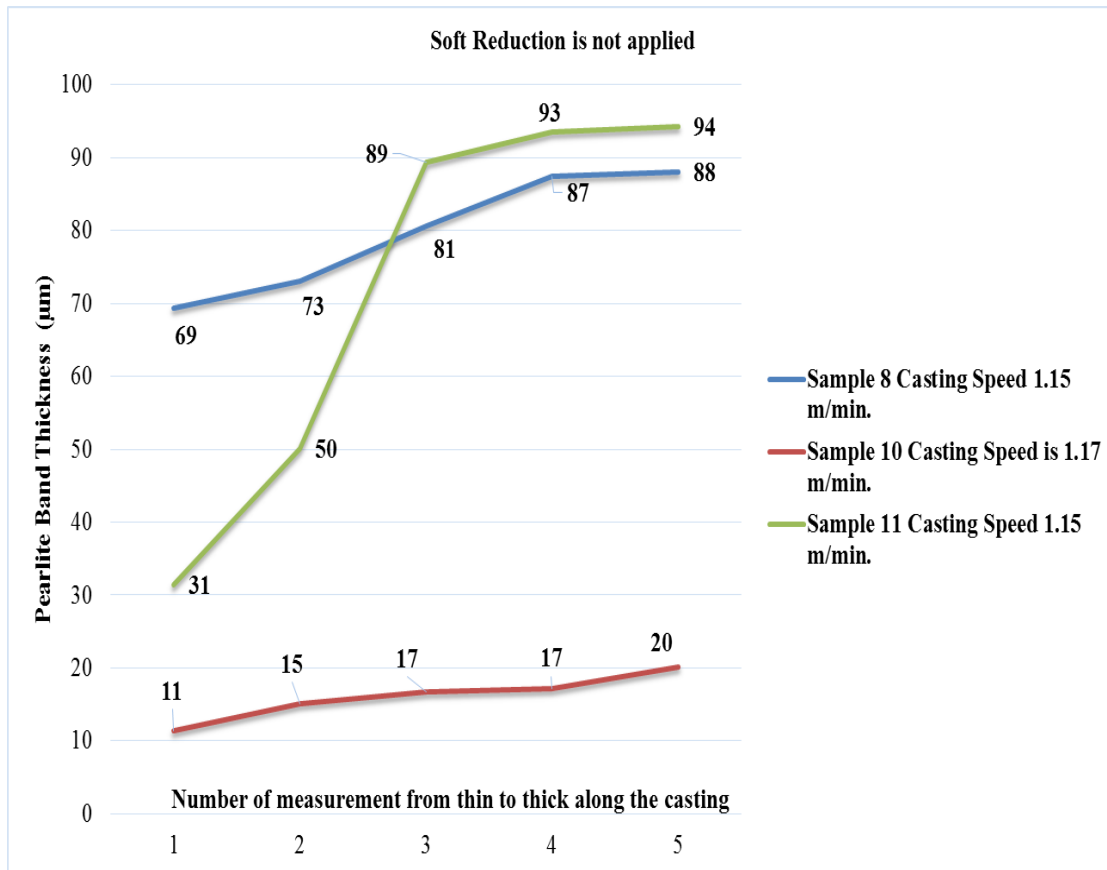
Figure 4.43 Soft Reduction is not applied. The thickness variation of the samples 8, 10 and 11 along the pearlite band are larger than other samples. Soft reduction is applied on the half of the sample 10 and then de-activated because of sticking alarm. That is why the pearlite band thickness of sample 10 is smaller than the others. The variation difference can be seen clearly. Casting Speeds are written on the figure.

4.3) SEM Investigation Results
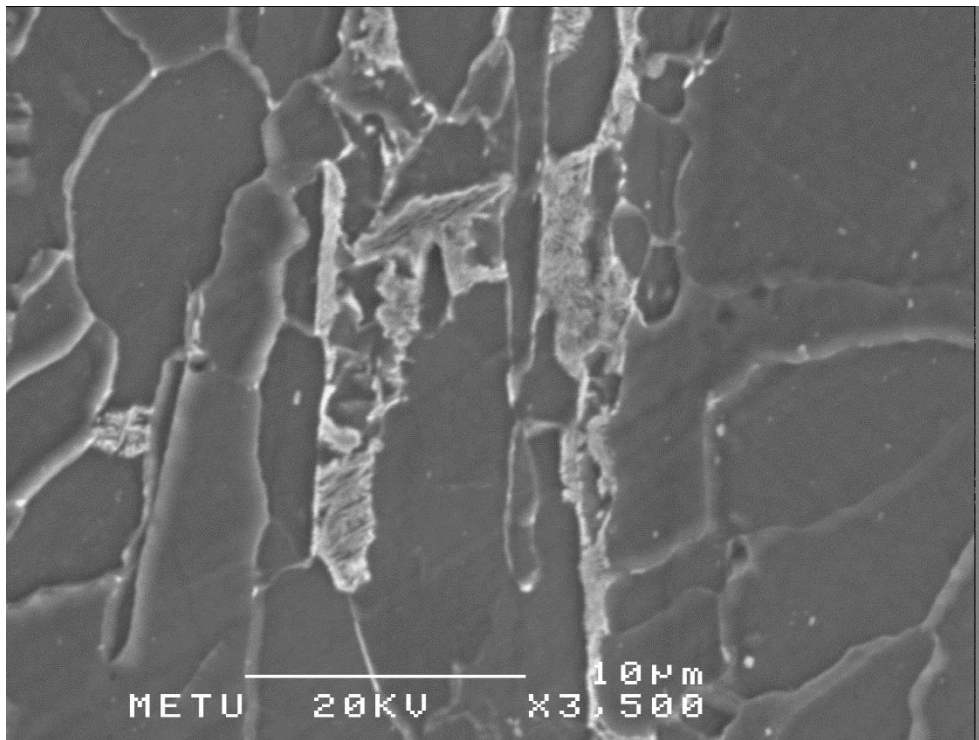
Figure 4.44 Sample 1 SEM Figure Soft Reduction Ratio is 1 mm/m.
Casting Speed is 1.15 m/min. Dispersed Pearlite Band
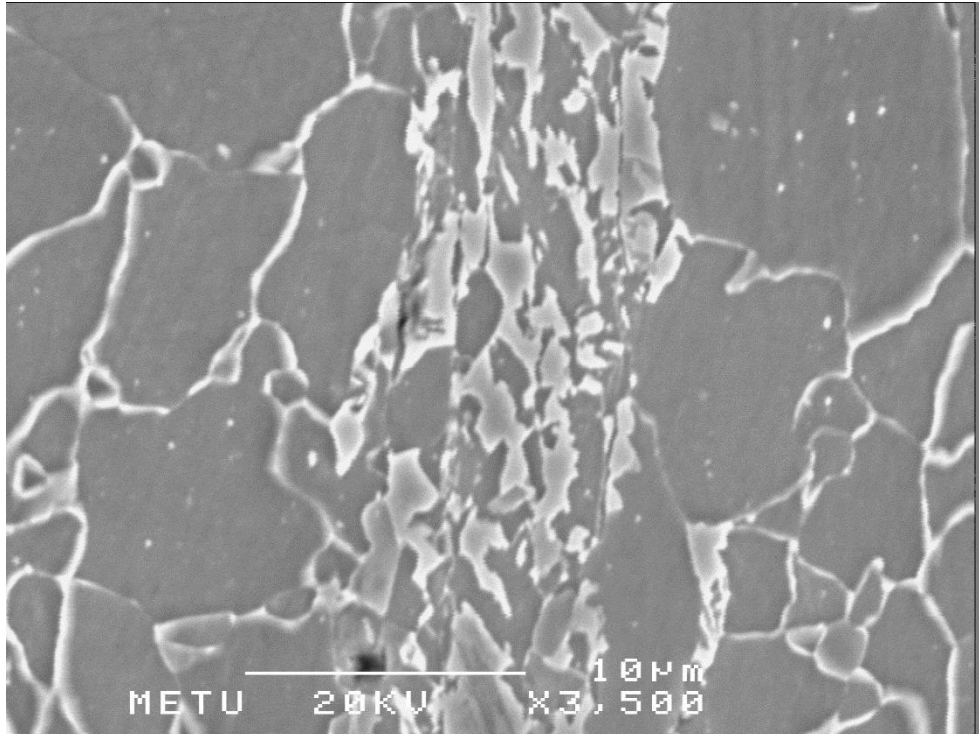
Figure 4.45 Sample 2 SEM Figure Soft Reduction Ratio is 1 mm/m.
Casting Speed is 1.05 m/min. Dispersed Pearlite Band
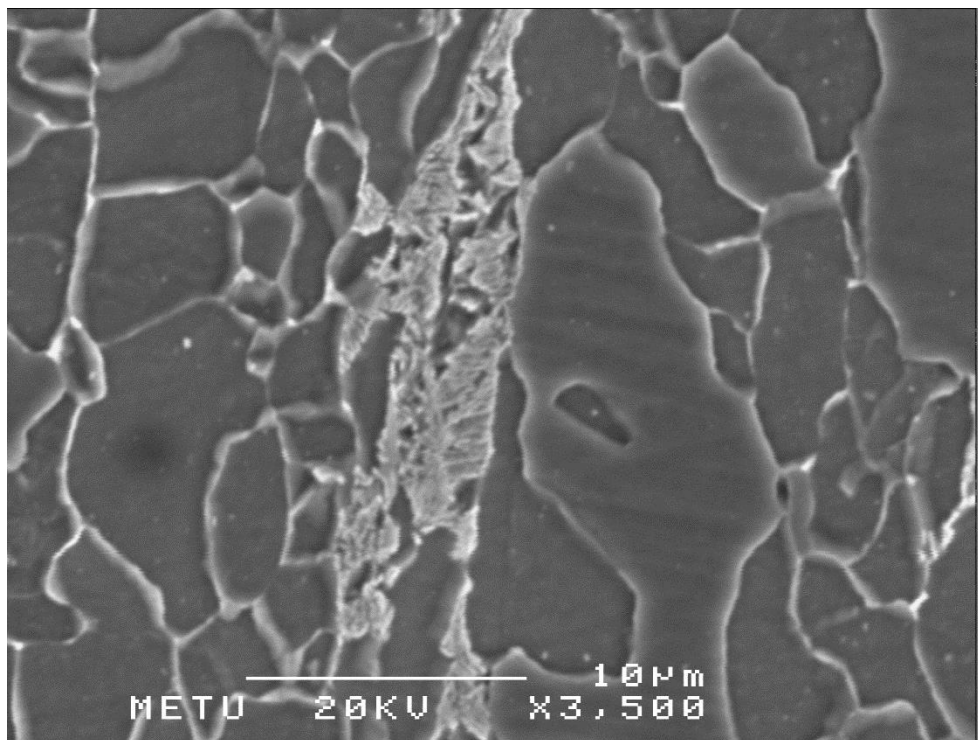
Figure 4.46 Sample 3 SEM Figure Soft Reduction Ratio is 1.00 mm/m. Casting Speed is 1.20 m/min. Sample 3 has one thin compact band.
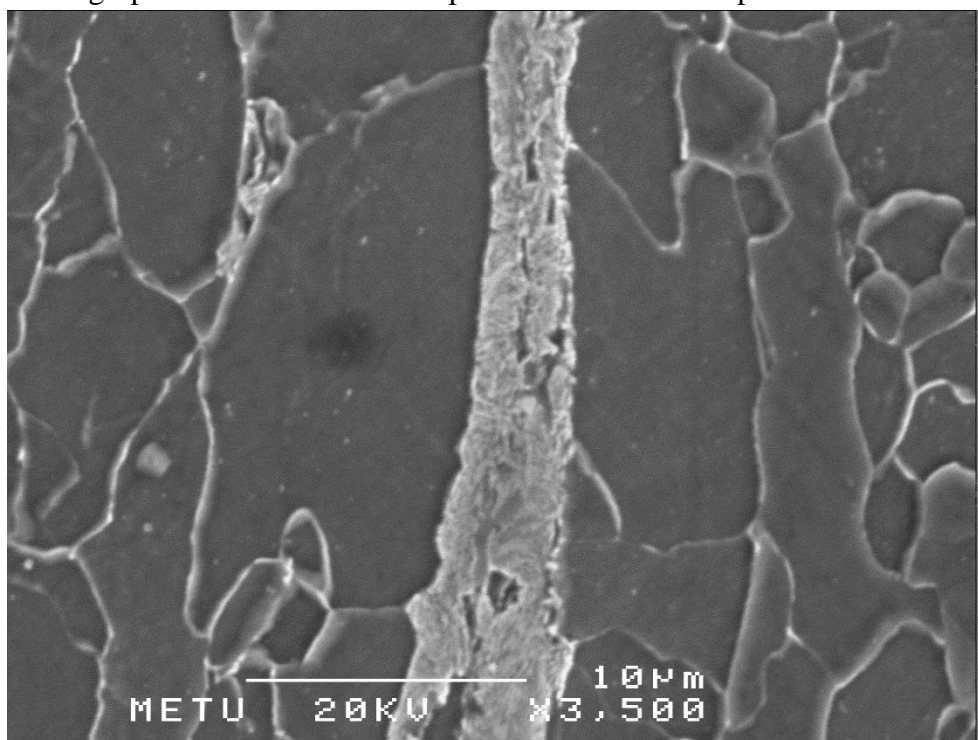
Figure 4.47 Sample 4 SEM Figure Soft Reduction Ratio is 1.00 mm/m. Casting Speed is 1.20 m/min. Sample 4 has one thin compact pearlite band.
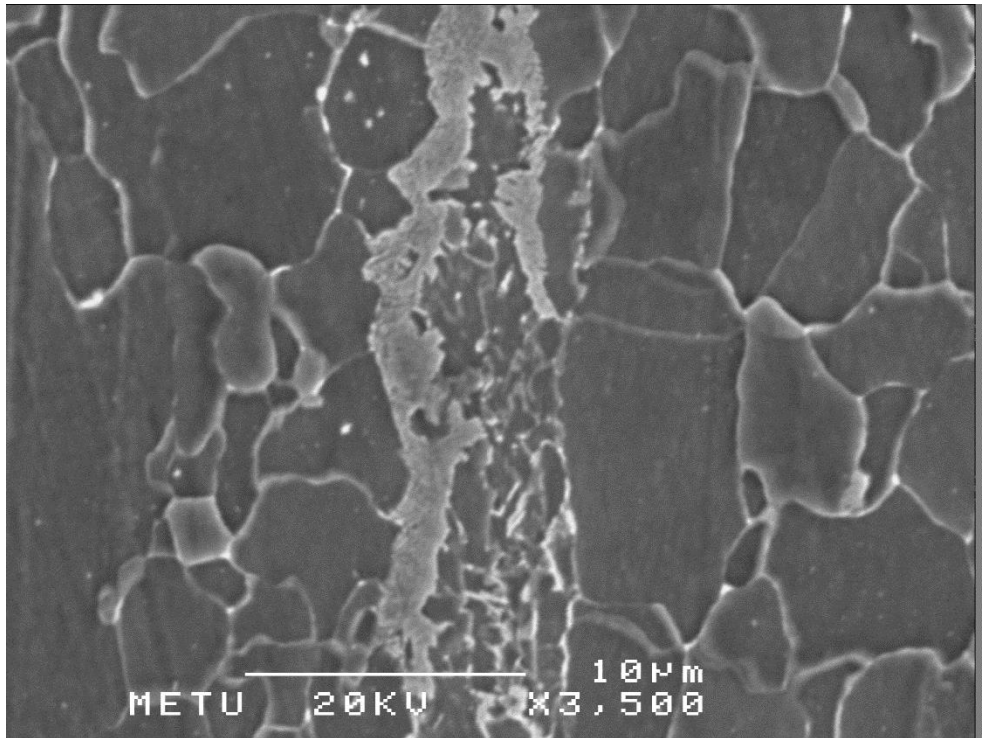
Figure 4.48 Sample 5 SEM Figure Soft Reduction Ratio is 1 mm/m.
Casting Speed is 1.20 m/min. Compact Pearlite Band
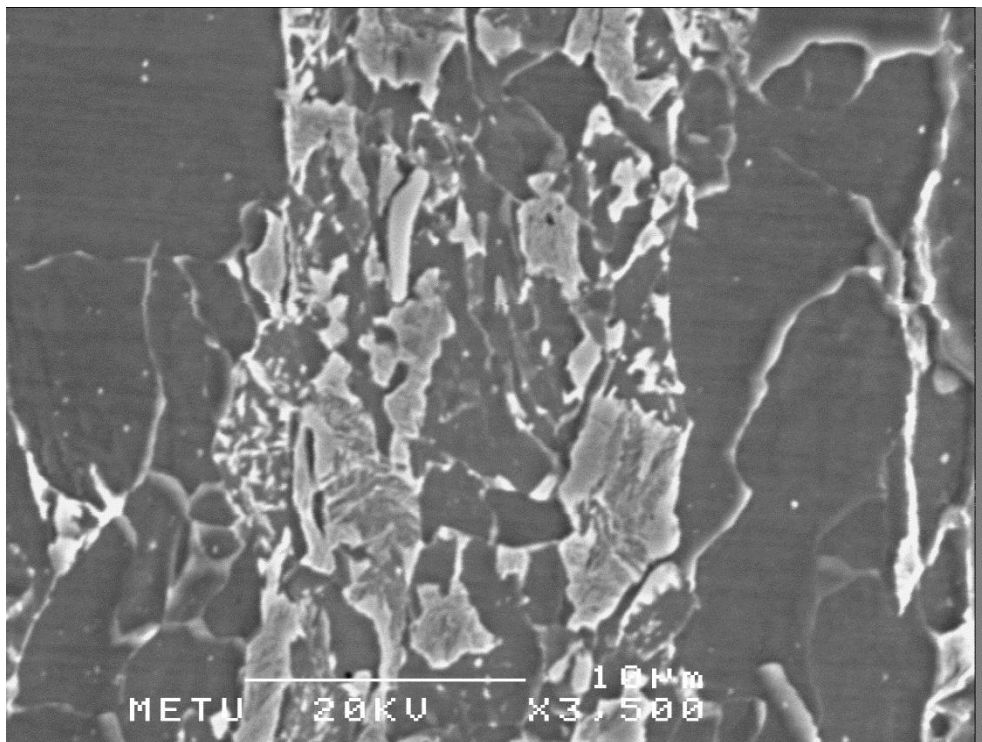
Figure 4.49 Sample 6 SEM Figure Soft Reduction Ratio is 1 mm/m.
Casting Speed is 1.15 m/min. Dispersed Pearlite Band
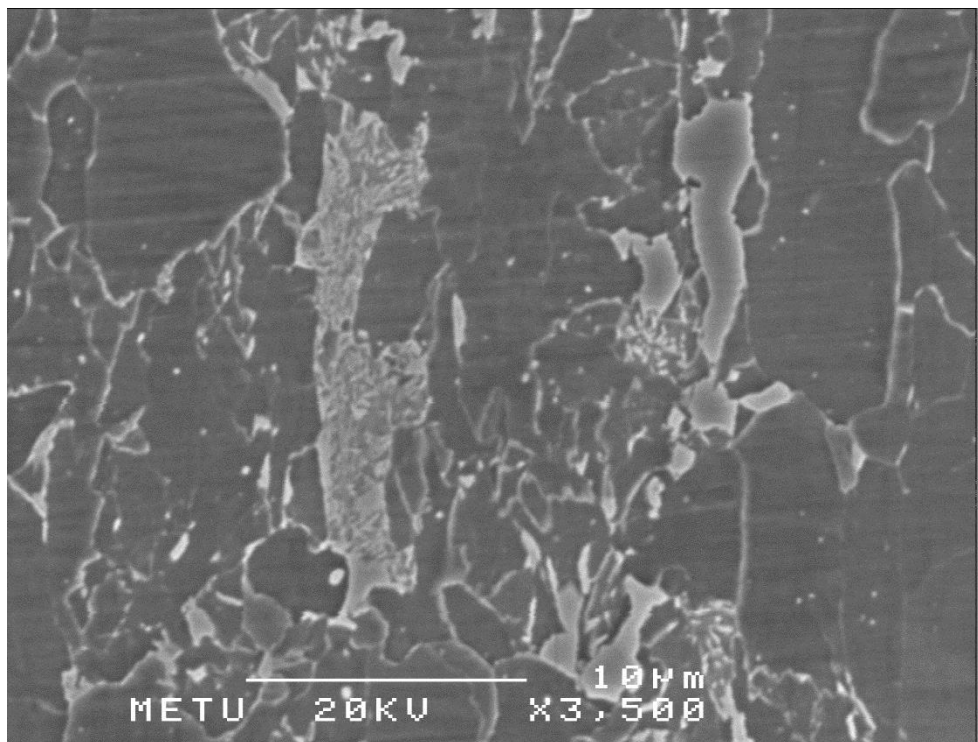
Figure 4.50 Sample 7 SEM Figure Soft Reduction Ratio is 1.10 mm/m.
Casting Speed is 1.15 m/min. Dispersed Pearlite Band
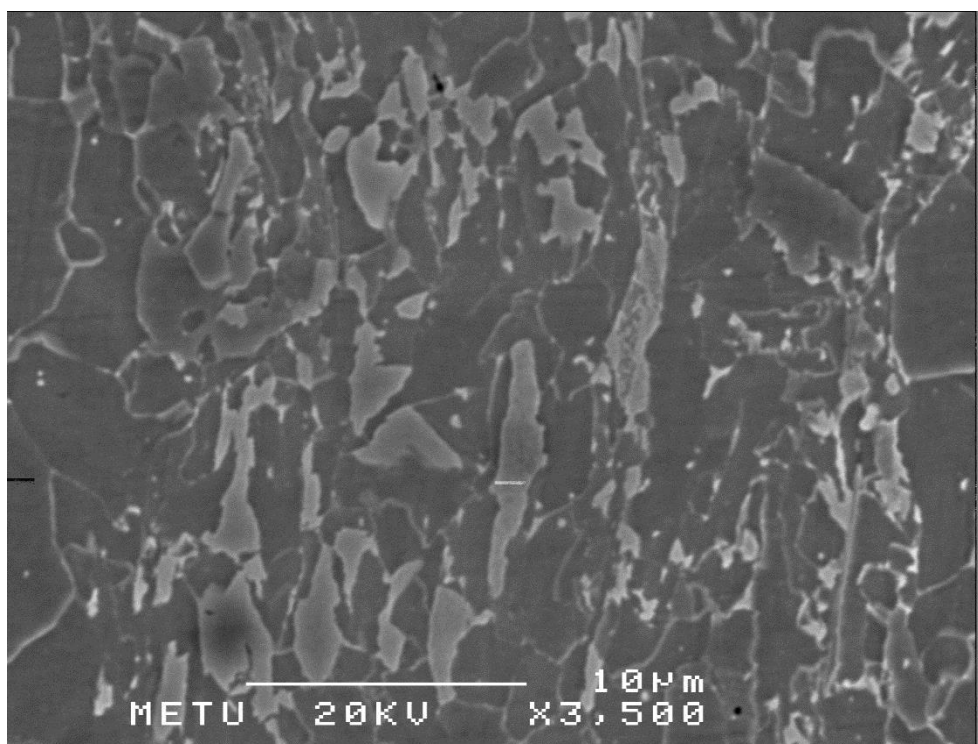
Figure 4.51 Sample 8 SEM Figure Soft Reduction is not applied
Casting Speed is 1.15 m/min. Dispersed Pearlite Band.
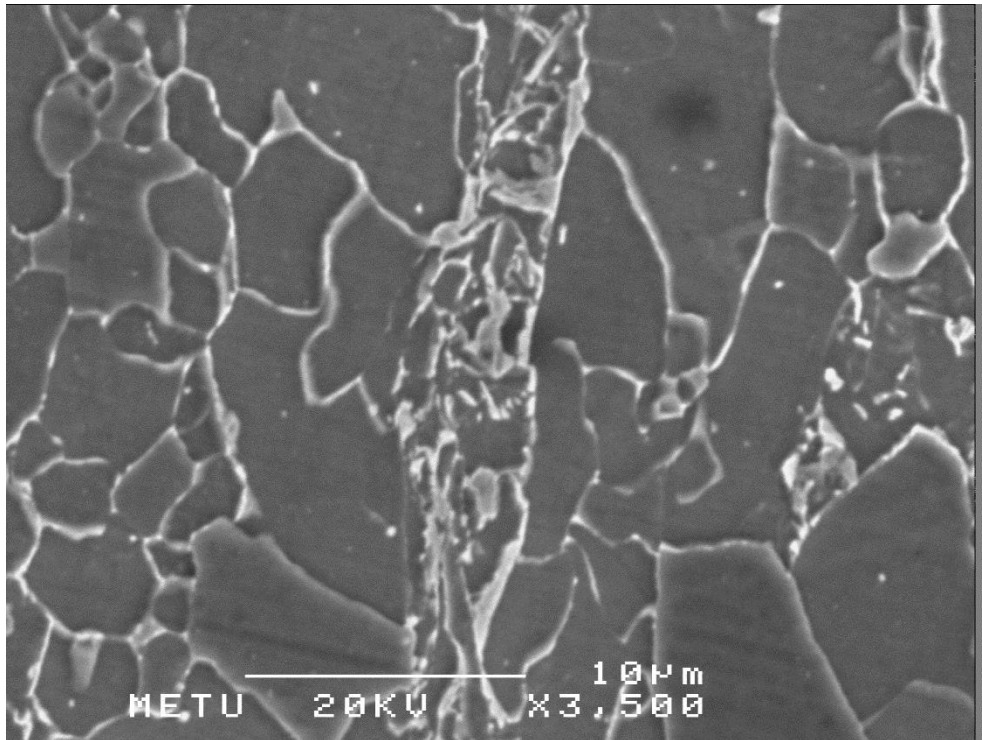
Figure 4.52 Sample 9 SEM Figure Soft Reduction Ratio is 1.20 mm/m.
Casting Speed is 1.15 m/min. Sample 9 has thin pearlite band consisting of
ferrite grains.
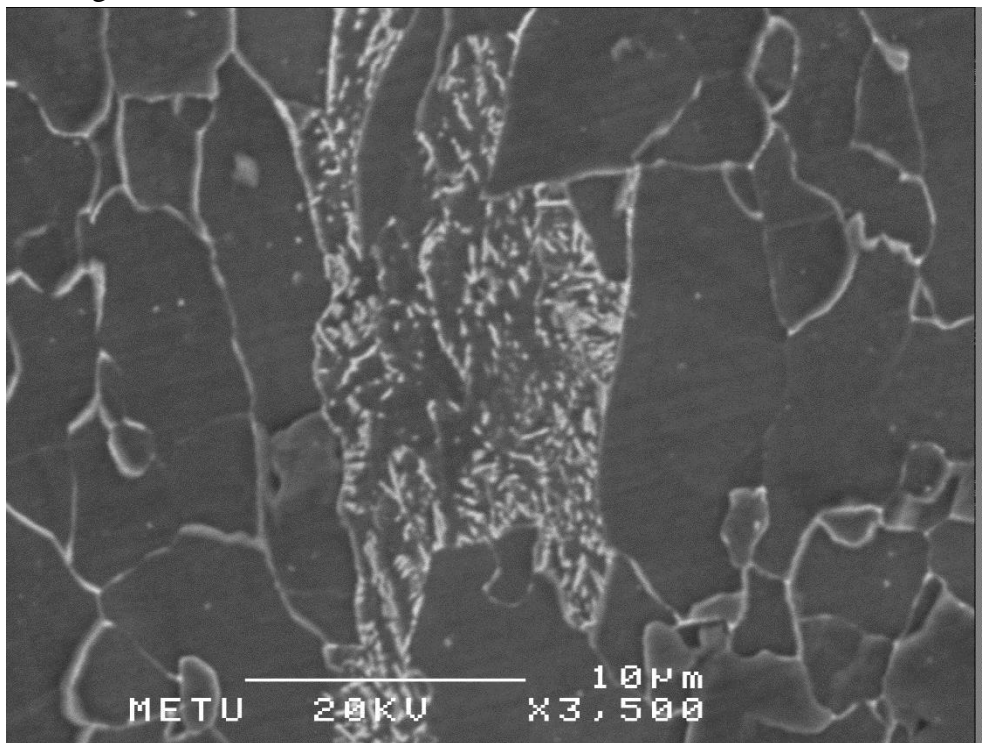
Figure 4.53 Sample 10 SEM Figure Soft Reduction is not applied
Casting Speed is 1.17 m/min. Dispersed Pearlite Band
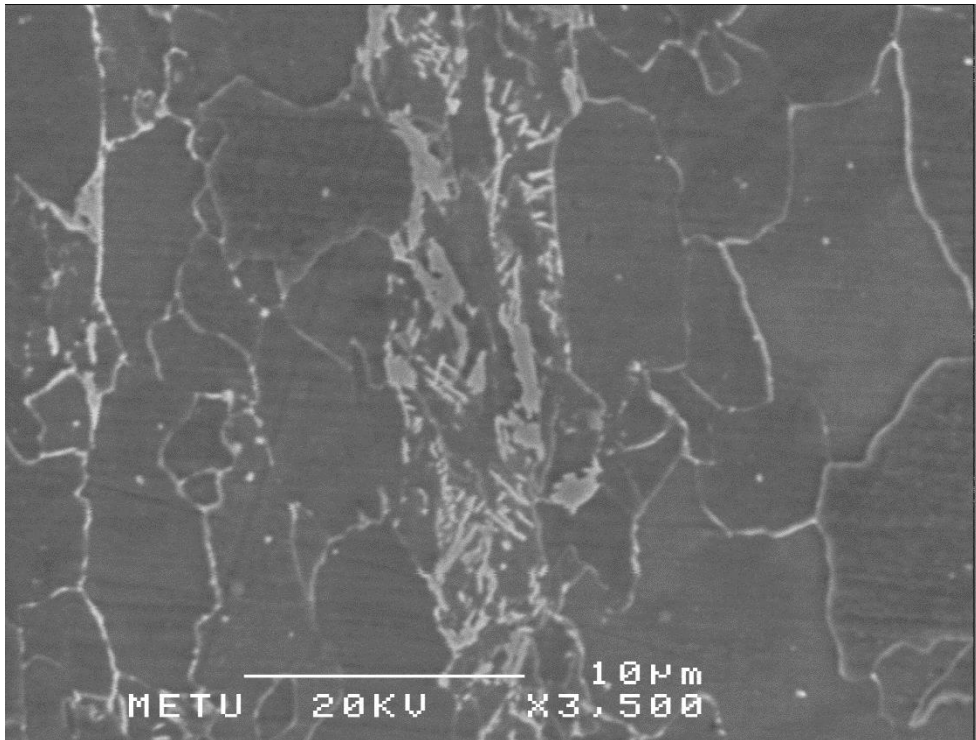
Figure 4.54 Sample 11 SEM Figure Soft Reduction is not applied
Casting Speed is 1.15 m/min. Dispersed Pearlite Band

The SEM microstructure figures were taken and EDS analysis was carried out on both pearlite and ferrite phase. In general view; the pearlite structure of the samples done by soft reduction was more compact than the samples without soft reduction. This fact is coherent with the microstructure figures. According to the literature; the soft reduction helps to eliminate the manganese segregation. To illustrate more clearly; soft reduction breaks the secondary dendrites which generally becomes manganese enriched in solute. By this way; manganese dissolves more uniformly in the solidified shell therefore pearlite band could be reduced.

4.4) Mechanical Testing Investigation Results

The main aim of investigating mechanical properties in this project is to study the effects of soft reduction on the mechanical properties of final product. The hot rolling temperatures are listed in Table 4.6. The hot rolling temperatures will be discussed later. To begin with the results of mechanical testing; after macro and micro structural investigation; the mechanical tests are applied to 11 coil samples regarding tensile testing, impact (charpy) energy testing, DWTT testing and micro hardness testing. To start with the tensile testing; according to the API X65 5L standard the minimum yield strength is 448 MPa and the minimum tensile strength is 531 MPa. The best result belongs to the sample 1 which is "0" segregation index. The yield and tensile strengths of sample 1 are 550 MPa and 630 MPa, respectively. The sample 1 almost satisfies the tensile strength requirement of API X80 that the yield and tensile strengths are 555 MPa and 621 MPa, respectively. However; the worst result belongs to the sample 3 which is also "0" segregation index. The yield and tensile strengths of sample 3 are 483 MPa and 568 MPa, respectively. This result satisfies the tensile strength requirement of API X60 steel grades. In general view; the best results belong to "0.5" segregation index samples. In other words; the average values of "0.5" segregation index are better than "1" and "0" segregation index samples. To be more specific; the sample 8 has the 518 MPa yield strength and 611 MPa tensile strength. The tensile strength result of sample 8; which has average 80 μm pearlite-ferrite band thickness, is better than the results of other samples.

Table 4.6 Hot Rolling Temperatures. The exit temperature of the reheating furnace is around 1200ºC. The passing number of the rough rolling is 7. The exit temperature of the rough rolling is around 1140ºC. The exit temperature of the fine rolling is around 810ºC. The temperature of coil rolling is around 540ºC.

Sample Number	Reheating Furnace Holding Time (Min)	Reheating Furnace Enter Temperature (°C)	Fine Rolling Enter Average Temperature (°C)
1	204	48	960-980
2	193	98	960-980
3	201	73	960-980
4	179	20	960-980
5	192	62	960-980
6	243	50	1010-1030
7	249	46	1010-1030
8	247	51	1010-1030
9	241	56	1010-1030
10	252	46	1010-1030
11	245	51	1010-1030

Table 4.7 Mechanical Testing Results. The coil thickness is 12.35 mm. The sample dimensions of the tensile testing is around 12 mm thickness and around 38 mm wide. The sample dimensions of the impact energy testing is 10x10x55 mm. The impact energy testing temperature is -10 ℃. The DWTT testing temperature is 0℃. The hardness testing type is HV 5.

#	Tensile Testing Results			Impact Energy Testing Results			DWTT Testing Results	Hardness Testing Results
	Yield Strength (MPa)	Ultimate Tensile Strength (MPa)	Elongation (%)	Sample-1(J)	Sample-2(J)	Sample-3(J)	DWTT (%)	Value (HV 5)
1	550	630	36	186	232	246	90	200
2	501	573	42	202	233	203	90	214
3	483	568	40	214	193	194	90	201
4	501	587	40	210	191	207	95	204
5	503	577	38	175	247	253	90	201
6	500	587	46	268	226	232	100	188
7	529	610	38	214	221	261	100	211
8	518	612	36	263	280	261	100	247
9	541	616	38	248	226	244	95	195
10	520	592	40	217	216	222	97	212
11	512	602	38	233	205	216	96	188

✓ Soft reduction is 1 mm/ meter and casting speed is 1.20 m/ min. for Sample 3, 4 and 5 and segregation is minimum. However; mechanical properties are worse than the other samples.

✓ Soft reduction is not applied and casting speed is 1.15 m/ min. for sample 8 and the best mechanical properties belongs to sample 8. Because the yield to tensile strength ratio is minimum.
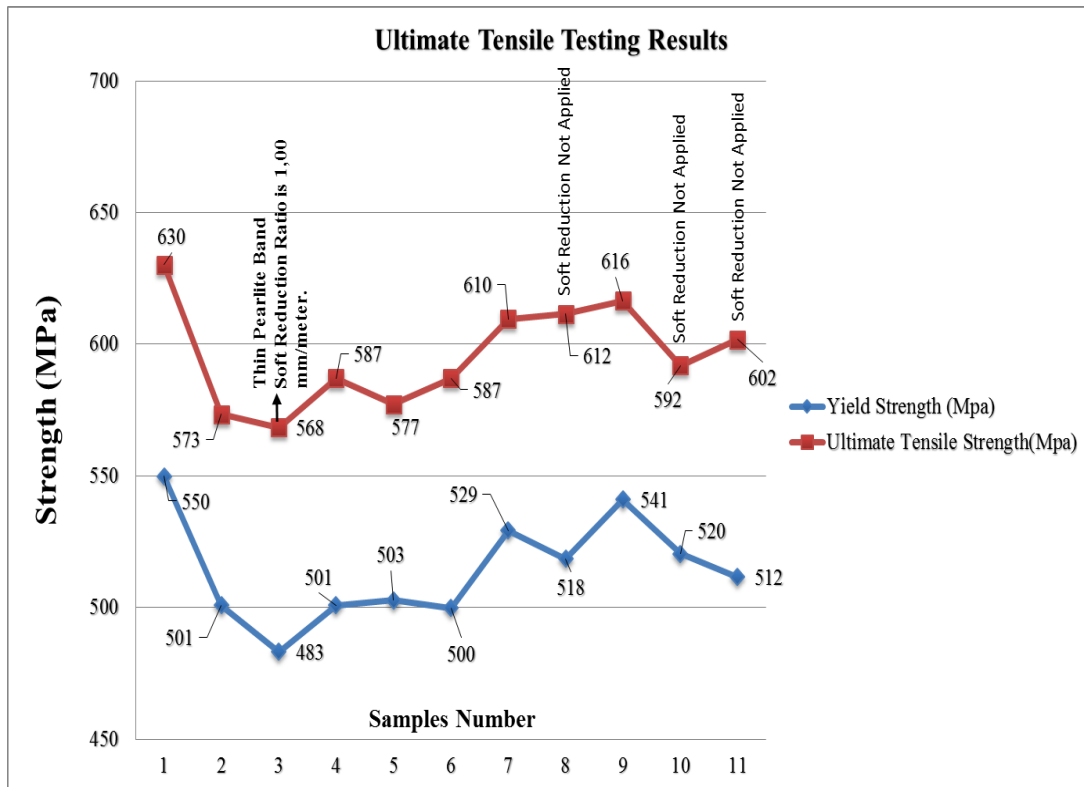
Figure 4.55 The Tensile Testing Results. The soft reduction is not applied to the sample 8, 10 and 11. The sample 3 has thinnest pearlite band thickness. The soft reduction ratio of sample 3 is 1 mm/m. The casting speed is 1.20 m/min. However; Sample 8, 10 and 11 are higher tensile testing results than sample 3.

Table 4.8 Yield to Tensile Strength Ratio

Sample Number	1	2	3	4	5	6	7	8	9	10	11
Yield to Tensile Ratio	0,872	0,874	0,850	0,853	0,871	0,851	0,868	0,848	0,878	0,879	0,850

Regarding the strain hardening; according to the API 5L standard the yield to tensile strength ratio should be less than 0.93 [31]. The best result belongs to sample 8 and the highest result belongs to sample 10.

Secondly; according to the API 5L X65 steel grades the impact energy should be minimum 27 joule at 0°C that can be achieved easily. However; the higher values for impact energy are the better results for pipes. One of the most important points here is the temperature because these kinds of petroleum and natural gas pipes are used in very tough environments such as -20°C. In this research the impact energy values were calculated at -10° C. The highest result belongs to the sample 8 which has average 268 Joule at -10°C. On the other hand; the lowest result belongs to sample 3 which has average 200 Joule at -10°C. The interesting point here is that sample 3 has the thinnest pearlite-ferrite band around 8 μm and sample 8 has the thickest pearlite-ferrite band around 83 μm.

Thirdly; although according to the API X65 5L standard 85 % result is accepted for the DWTT test; 100 % results are expected from these steel grades after hot rolling process because X65 steel grades are used in tough conditions. Another interesting point in this research is that the 100 % DWTT test results belong to the "0.5" segregation index samples. On the contrary; the 90 % DWTT test results belong to the "0" segregation index. Finally; regarding Vickers hardness test 2 times from both surfaces was applied to the samples. The average results are listed in Table 2.4. According to the API 5L standard; the maximum value should be 350 HV. All the Vickers hardness test results of the samples were under the desired result.

In general view; as it can be seen obviously that the sample 8; which has the thickest pearlite-ferrite band, has the best mechanical properties. On the contrary; sample 3; which has the thinnest pearlite-ferrite band, has the lowest mechanical properties. Concerning the hot rolling temperatures; the exit temperature of the reheating temperature, rough rolling and fine rolling were the same for all samples. The only difference of sample 1,2,3,4 and 5 comes from the entering temperature of the fine rolling. In other words; the cooling speed of sample 1,2,3,4 and 5 between the exit of rough rolling and enter of fine rolling is faster than the other samples. This fast cooling determines the morphology of the ferrite such as quasi-ferrite, polygonal ferrite etc. For instance; according to the previous researches; the morphology of the ferrite strictly determines the mechanical properties. Therefore; the morphology of the ferrite depends on the hot rolling parameters. Consequently; it can be inferred that the soft reduction does have any effect on the mechanical properties.

CHAPTER 5

CONCLUSIONS

Regarding elimination of pearlite-ferrite band using soft reduction of API 5L X65 steels during continuous casting in the present study; the following major conclusions have been drawn;

1) The soft reduction is definitely the effective method to reduce the pearlite-ferrite bands formed during continuous casting. In the zero strength region of the solidified shell dendrites are broken using soft reduction. This makes the alloying elements disperse more uniformly and pearlite band reduced from average 80 μm to 11 μm during continuous casting.

2) Considering the constant metallurgical length, casting speed and soft reduction ratio; the optimum soft reduction ratio is 1 mm/m. for 1.20 m/min. for API X65 steel grade.

3) The solid wall thickness of the slab during continuous casting using soft reduction is important parameter because there should be required time to fill the liquid into the casting cavities. To determine the soft reduction ratio for any steel grade the solid wall thickness of the slab should be considered carefully.

4) The soft reduction does not have any effect on the mechanical properties of coils. The rolling parameters play major role on the mechanical properties of coils.

5) Soft reduction does not have any effect on the grain size.

6) Regarding the convection, conduction methods and SMS Demag program, at the exit of the mold the thickness of the slab is 15.92 mm, 32 mm and 17.37 mm; respectively. The required mold cooling water regarding conduction and SMS Demag program are 2171 kg/min and 2400 kg/min; respectively. Comparing the mathematical calculations and SMS Demag software program, the convection method is more correct to determine the metallurgical length and the conduction method is more suitable to determine the required cooling water for the mold.

7) The heat transfer coefficient in the mold was re-calculated using the convection heat transfer model based on the mold cooling water. During experiments the mold cooling water was 3900 kg/min. The calculated heat transfer coefficient was 2727 W/m^2K. In next step; the solidified thickness of the slab at the exit of the mold was calculated as 22 mm which is very close to the thickness calculated by SMS Demag Program during continuous casting.

CHAPTER 6

SUGGESTIONS FOR FUTURE WORK

1) The dendrite and equiaxed solidified regions of the slab macro samples can be measured.

2) The soft reduction can be applied on 2 segments at the same time. By this way; the effect of the soft reduction can be seen.

3) Either reheating time or temperature can be increased to increase the manganese diffusion.

REFERENCES

1. Mikio Suzuki; and Yuichi Yamaoka, "Influence of Carbon Content on Solidifying Shell Growth of Carbon Steels at the initial stage of solidification", 2003, Materials Transactions, Volume 44 (5) : pp. 836-844.

2. B.A.Sivak.,G.Grachev,V.M.Parshin,A.D.Chertov,S.V.Zarubin,V.G.Fisenko,"Mhd Processes in the electromagnetic stirring of liquid metal in continuous section and Bloom Casters", 2009, Metallurgist 1: pp. 537-538.

3.Ted. F. Majka, David K. Matlock, George Krauss, "Development of Microstructural Banding in Low-Alloy Steel with Simulated Mn Segregation", 2007, Metallurgical and Materials Transactions A Volume 33: pp. 1627-1633.

4.K. Miłkowska-Piszczek, M. Dziarmagowski, A. Buczek, J. Pióro, "The methods of calculating the solidifying strand shell thickness in a continuous casting machine", 2012, Archives of Materials Science and Engineering Volume 57 (2): pp. 75-79.

5.Kristin Carpenter, "The influence of micro alloying elements on the hot ductility of thin slab cast steel", 2004, PhD Thesis, Department of Materials Engineering, University of Wollongong.

6. Michael Korchynsky, "Strategic Importance of Thin Slab Casting Technology", 2002, The International Symposium on Thin-Slab Casting and Rolling in Guangzhou China.

7. Rogerio Augusto Carneiro, Rajindra Clement Ratnapuli, Vanessa de Freitas Cunha Lins, "The influence of chemical composition and microstructure of API linepipe steels on hydrogen induced cracking and sulfide stress corrosion cracking", 2003, Materials Science and Engineering A Volume 357: pp.104-110.

8. Mingzhong Liu, J. L., "Application of soft reduction technology in continuous-casting billet", 2004, Journal of University of Science and Technology Beijing, pp. 302-306.

9. Mujun Long, Dengfu Chen, "Study on Mitigating Center Macro-Segregation during Steel Continuous Casting Process", 2011, Steel Research Institute 82-7: pp. 847-858.

10. American Petroleum Institute, "Specification for Line Pipe ANSI/API Specification", 2008.

11.L.W. Stay, Y.C. Chen, S.L.I. Chan, "Sulfide Stress Corrosion Cracking and Fatigue Crack Growth of Welded TMCP API 5L X65 pipe-line steel", 2001, International Journal of Fatigue Volume 23, pp. 103-113.

12. Ricardo Biniscius B. Gomes, Cicero Humberto Aidar, Sergio Seijo Kojima, "Study of the mechanics fracture in API 5L X70 and X70 steel pipes", 2012, Tenaris ConFab Company.

13. A.Fragiel, R. Schouwenaarf, R. Guardian, R. Perez, "Microstructural Characteristics of Different Commercially Available API 5L X65 Steels", 2005, Journals for Electrochemical Systems Volume 8: pp. 115-119.

14. Chang-Kyun Oh, Yun-Jae Kim, Jong- Hyun Baek, Young-Pyo Kim, Woo-Sik Kim, "Ductile failure analysis of API X65 pipes with notch-type defects using a local fracture criterion", 2007, International Journal of Pressure Vessels and Piping Volume 84: pp. 512-525.

15. Ali Kalkanlı, "Lecture Notes of Near Net Shape Casting", 2004.

16. SMS Demag Technology Manuel, 2008.

17. Mingzhong Liu, Jingshe Li, Shiqi Li, Hongjun Yan, Yingjun Fan, Mingshen Yang, "Application of soft reduction technology in continuous-casting billet", 2004, Journal of University of Science and Technology Beijing 11-4: pp. 302-310.

18. Liu Ke, Chang Yun-he, Han Zhang-guang, Zhang Jia-quan, "Effect of Asynchronous Adjustments of Clamping Cylinders on Triangular Crack of Slab Castings Under Application of Soft Reduction", 2013, Journal of Iron and Steel Research 20-2: pp. 38-47.

19. Ke Liu, Jiaquan Zhang, "Numerical Analysis of Optimum Soft Reduction amount for continuous casting slab", 2012, Metallurgia International 17-4: pp. 14-20.

20. Deep Samanta, Nicholas Zabaras, "Control of macrosegregation during the solidification of alloys using magnetic fields", 2006, International of Heat and Mass Transfer Volume 49: pp. 4850-4866.

21. C.Beckermann, M.C.Schneider, "Simulation of Convection and Macrosegregation in Steel Casting", 1996, SFSA Technical and Operating Conference 4-2.

22. Einar Haug, Asbjqrn Mo, Havard J. Thevik, "Macrosegregation near a cast surface caused by exudation and solidification shrinkage", 1995, Journal of Heat and Mass Transfer Volume 8-9: pp.1553-1563.

23. G. Lesoult, "Macrosegregation in steel strands and ingots Characterisation Formation and Consequences", 2005, Materials Science and Engineering A Volume 413-414: pp. 19-29.

24. C.P.Reip,S.Shanmugam, R.D.K. Misra, "High strength microalloyed CMn(V–Nb–Ti) and CMn(V–Nb) pipeline steels processed through CSP thin-slab technology Microstructure Precipitation and Mechanical Properties,", 2006, Materials Science and Engineering A Volume 424: pp. 307-317.

25. R.I.L Guthrie, R.P. Tavares; "Mathematical and physical modelling of steel flow and solidification in twin roll horizontal belt thin strip casting machines", 1997, International Conference on CFD in Mineral and Metal Processing and Power Generation.

26. N.Narasaiah, K.K. Ray, "Small crack formation in a low carbon steel with banded ferrite pearlite structure", 2005, Materials Science and Engineering A 392: pp. 269-277.

27. Y.D. Huang, L. Froyen, "Important factors to obtain homogeneous and ultrafine ferrite pearlite microstructure in low carbon steel", 2002, Journal of Materials Processing Technology Volume 124: pp. 216-226.

28. L.Tau, S.L.I. Chan, "Effects of ferrite pearlite alignment on the hydrogen permeation in a AISI 4130 steel", 1996, Materials Letters Volume 29: pp. 143-147.

29. G. Laschet, P. Fayek, T.Henke, H.Quade, U. Prahl, "Derivation of anisotropic flow curves of ferrite–pearlite pipeline steel via a two level homogenisation scheme", 2013, Materials Science and Engineering A Volume 566, pp. 143-156.

30. V.I. Spivakov, E.A. Orlov, P.L.Litvinenko, A.V.Nogovitsyn, "Kinetics of Austenite Transformation and Bainite Structure Formation during strain hardening of low pearlite steel X 70 plates for Gas Pipelines", 2010, Metallurgical and Mining Industry 2-1, pp. 39-42.

31. B.G. Thomas, "Continuous Casting", 2001, The Encyclopedia of Materials: Science and Technology Volume 2: pp. 1595-1599.

32. B.G. Thomas, G.Li, A.Moitra, D.Habing, "Analysis of Thermal and Mechanical Behavior of Copper Molds during Continuous Casting of Steel Slabs", 1997, 80th Steel Making Conference April, pp. 13-16.

33. T. Kajitani, J.M. Drezet, M. Rappaz, "Numerical Simulation of Deformation-Induced Segregation in Continuous Casting of Steel", 2001, Metallurgical and Materials Transactions A Volume 32: pp. 1479 1512.

34. C.Gheorghies, I.Crudu, C. Teletin, C. Spanu, "Theoretical Model of Steel Continuous Casting Technology", 2001, Journal of Iron and Steel Research Volume 16-1: pp. 12-16.

35. ASTM International, "ASTM Steel Handbook: High Strength Low Alloy Steels", 2009, pp. 196-245.

36. A.W.D Hills, M.R.Moore, "The solidification of pure metals (and eutectics) under uni-directional heat flow conditions: II. Solidification in the presence of superheat", 1975, Metallurgical and Material Transactions 6B: pp. 131-138.

37. SMS Demag, "Dynamic Solidification Control Software Program", 2008.

38. S.Luo, M.Y.Zhu, C.Ji, Y.Chen, "Characteristics of solute segregation in continuous casting bloom with dynamic soft reduction and determination of soft reduction zone", 2010, Iron and Steel Making Volume 37-2: pp. 141-146.

39. S. Mazumdar, S.K.Ray; "Solidification control in continuous casting of steel", 2001, Sadhana Volume 26: pp. 179-198.

40. K. Kim, T.Yeo, K.H. Oh, D.N.Lee, "Effect of Carbon and Sulfur in continuously cast strand on longitudinal surface cracks", 1996, ISIJ International Volume 36: pp. 284-289.
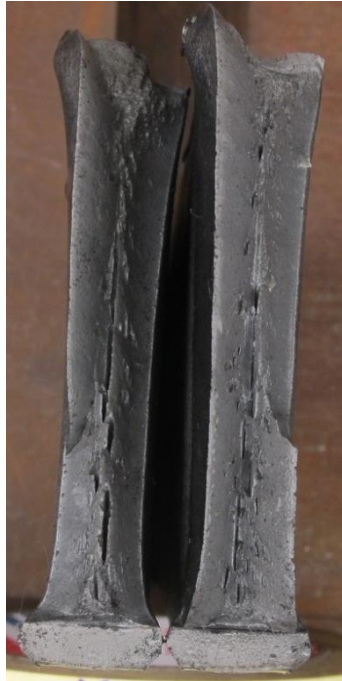
APPENDIX A

DWTT FIGURES

Figure A.1 Sample 1
Soft Reduction Ratio is 1 mm/m.
Casting Speed is 1.15 m/min.

Figure A.2 Sample 2
Soft Reduction Ratio is 1 mm/m.
Casting Speed is 1.05 m/min.

Figure A.3 Sample 3
Soft Reduction Ratio is 1 mm/m.
Casting Speed is 1.20 m/min.

Figure A.4 Sample 4
Soft Reduction Ratio is 1 mm/m.
Casting Speed is 1.20 m/min.

Figure A.5 Sample 5
Soft Reduction Ratio is 1 mm/m.
Casting Speed is 1.20 m/min.

Figure A.6 Sample 6
Soft Reduction Ratio is 1 mm/m.
Casting Speed is 1.15 m/min.

Figure A.7 Sample 7
Soft Reduction Ratio is 1.10 mm/m.
Casting Speed is 1.15 m/min.

Figure A.8 Sample 8
Soft Reduction is not applied.
Casting Speed is 1.15 m/min.

Figure A.9 Sample 9
Soft Reduction Ratio is 1.20 mm/m.
Casting Speed is 1.15 m/min.

Figure A.10 Sample 10
Soft Reduction is not applied.
Casting Speed is 1.17 m/min.

Figure A.11 Sample 11 Soft Reduction is not applied.
Casting Speed is 1.15 m/min.
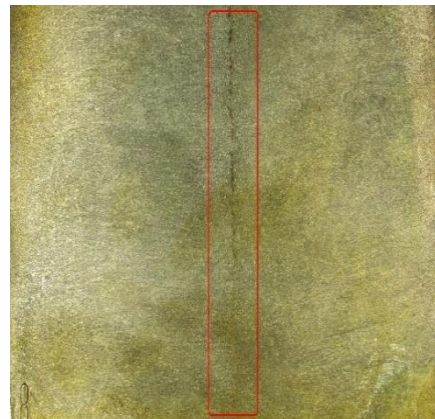
APPENDIX B

MACRO STRUCTURE FIGURES

Figure B.1 Macro Sample 2 Side 3
Soft Reduction Ratio is 1 mm/m.
Casting Speed is 1.05 m/min.

Figure B.2 Macro Sample 2 Side 4
Soft Reduction Ratio is 1 mm/m.
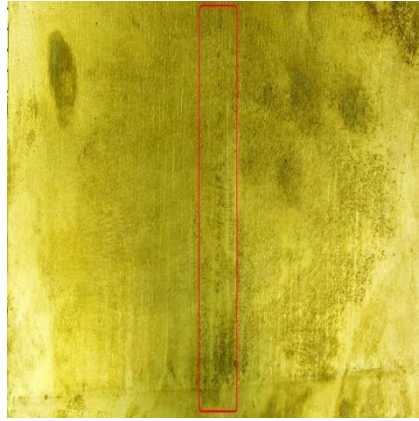Casting Speed is 1.05 m/min.

Figure B.3 Macro Sample 4 Side 3
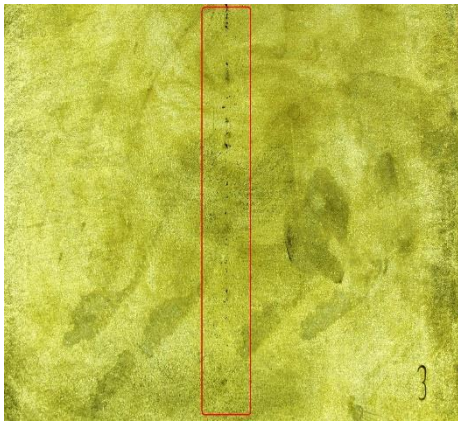Soft Reduction Ratio is 1 mm/m.
Casting Speed is 1.20 m/min.

Figure B.4 Macro Sample 4 Side 4
Soft Reduction Ratio is 1 mm/m.
Casting Speed is 1.20 m/min.

Figure B.5 Macro Sample 5 Side 3
Soft Reduction Ratio is 1 mm/m.
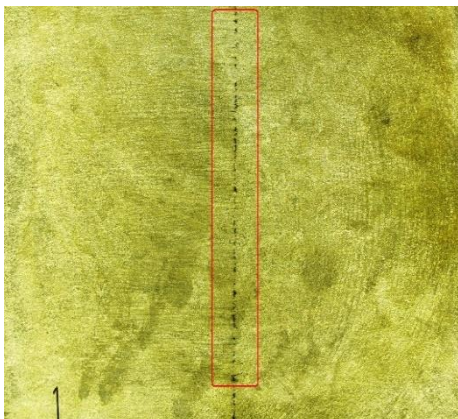Casting Speed is 1.20 m/min.

Figure B.6 Macro Sample 5 Side 4
Soft Reduction Ratio is 1 mm/m.
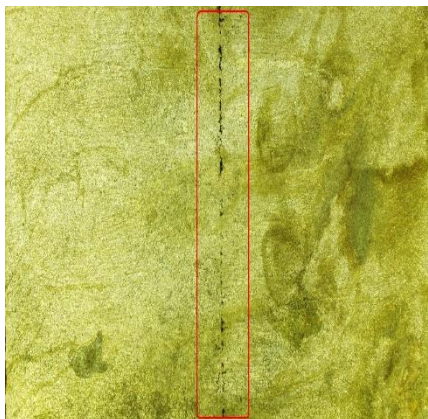Casting Speed is 1.20 m/min.

Figure B.7 Macro Sample 9 Side 3
Soft Reduction Ratio is 1.20 mm/m.
Casting Speed is 1.15 m/min.

Figure B.8 Macro Sample 9 Side 4
Soft Reduction Ratio is 1.20 mm/m.
Casting Speed is 1.15 m/min.

Figure B.9 Macro Sample 10 Side 3
Soft Reduction is not applied.
Casting Speed is 1.17 m/min.

Figure B.10 Macro Sample 10 Side 4
Soft Reduction is not applied.
Casting Speed is 1.17 m/min.